

3D Biomimetic Models to Reconstitute Tumor Microenvironment In Vitro: Spheroids, Organoids, and Tumor-on-a-Chip

Wenxiu Li, Zhihang Zhou, Xiaoyu Zhou, Bee Luan Khoo, Renardi Gunawan, Y. Rebecca Chin, Liang Zhang, Changqing Yi, Xinyuan Guan, and Mengsu Yang*

Decades of efforts in engineering in vitro cancer models have advanced drug discovery and the insight into cancer biology. However, the establishment of preclinical models that enable fully recapitulating the tumor microenvironment remains challenging owing to its intrinsic complexity. Recent progress in engineering techniques has allowed the development of a new generation of in vitro preclinical models that can recreate complex in vivo tumor microenvironments and accurately predict drug responses, including spheroids, organoids, and tumor-on-a-chip. These biomimetic 3D tumor models are of particular interest as they pave the way for better understanding of cancer biology and accelerating the development of new anticancer therapeutics with reducing animal use. Here, the recent advances in developing these in vitro platforms for cancer modeling and preclinical drug screening, focusing on incorporating hydrogels are reviewed to reconstitute physiologically relevant microenvironments. The combination of spheroids/organoids with microfluidic technologies is also highlighted to better mimic in vivo tumors and discuss the challenges and future directions in the clinical translation of such models for drug screening and personalized medicine.

1. Introduction

Cancer is one of the major causes of death worldwide and seriously threatens the health of human beings. In 2020, an estimated 19.3 million new cancer cases and around 10 million cancer-related deaths were reported across the globe.^[1] The high incidence and mortality of cancer make it urgent to develop more effective cancer therapeutics. The success rate of anticancer drug candidates during clinical screening is extremely low, with less than 4% passing through clinical trials to obtain FDA approval, mainly due to their side effects and deficiency in efficacy.^[2] A vital cause behind the high attrition rates of most candidate therapeutics is the lack of preclinical models that enable comprehensively mimicking tumor inherent complexity and heterogeneity. This problem raises a high demand to design more reliable and predictive preclinical models for improving the efficiency of drug development and deciphering the mechanism of cancer biology.

The 2D monolayer culture models have been widely utilized as prescreening tools to evaluate the efficacy and safety of potential

W. Li, X. Zhou, B. L. Khoo, R. Gunawan, Y. R. Chin, L. Zhang, M. Yang
Department of Precision Diagnostic and Therapeutic Technology
City University of Hong Kong Shenzhen Futian Research Institute
Shenzhen 518000, China
E-mail: bhmyang@cityu.edu.hk


W. Li, Z. Zhou, X. Zhou, R. Gunawan, Y. R. Chin, L. Zhang, M. Yang
Department of Biomedical Sciences
Tung Biomedical Sciences Centre
City University of Hong Kong
Hong Kong, SAR 999077, China

Z. Zhou
Department of Gastroenterology
the Second Affiliated Hospital of Chongqing Medical University
Chongqing 400010, China

B. L. Khoo
Department of Biomedical Engineering
City University of Hong Kong
Hong Kong 999077, China

C. Yi
Guangdong Provincial Engineering and Technology Center of Advanced
and Portable Medical Devices
School of Biomedical Engineering
Sun Yat-sen University
Guangzhou 518107, China

X. Guan
Department of Clinical Oncology
State Key Laboratory for Liver Research
The University of Hong Kong
Hong Kong, SAR 999077, China

 The ORCID identification number(s) for the author(s) of this article can be found under <https://doi.org/10.1002/adhm.202202609>

© 2023 The Authors. Advanced Healthcare Materials published by Wiley-VCH GmbH. This is an open access article under the terms of the Creative Commons Attribution-NonCommercial License, which permits use, distribution and reproduction in any medium, provided the original work is properly cited and is not used for commercial purposes.

DOI: 10.1002/adhm.202202609

anticancer drugs for over 100 years.^[3] Although 2D models are easy to use, high throughput, and cost-effective, they cannot recreate the complex interactions between tumor cells and the surrounding microenvironment within human bodies. Such is particularly evidenced by cancer cells cultured in 2D conditions undergoing different phenotypes,^[4] gene and protein expressions,^[5] and drug responses^[6] from those in vivo. Therefore, animal models remain a gold standard for drug screening and cancer research by offering a more complex and actual physiological microenvironment. Nevertheless, they provide only a murine physiology microenvironment for implanted human cells, lacking key characteristics of the human native organs, and biosystem functionalities. Moreover, the immune system of mice is generally compromised, which might influence cancer progression and reduce their reliability in drug testing.^[7] To address these issues, humanized mouse models have been recently created to investigate the crosstalk between cancer and human immune system through gene editing technology.^[8] However, such models are still unable to faithfully capture key aspects of the human tumor microenvironment (TME).^[9] In addition, animal models are cost-intensive, low throughput, and time-consuming. The high number of animals employed in laboratory research also raises ethical disputes. Thus, alternative approaches are required to better recapitulate in vivo TME in a more precise and clinical relevance manner.

To this end, 3D cell culture models such as spheroids are subsequently developed to replicate physiological microenvironment configurations partially. Furthermore, more complex organotypic cultures are proposed where self-assembled cellular organoids may capture the nature of tumors at an organ level.^[10] These static 3D models have provided a deeper insight into the mechanisms governing tumor progression and exhibited great potential in anticancer drug screening. However, owing to the lack of tissue-tissue interface, vasculature, and mechanical factors in the microenvironment (e.g., dynamic fluid flow), these 3D models are limited in capturing the cancer metastasis cascade, which are important cues in tumor control and progression.^[11] Additionally, the lack of a pre-existing matrix hinders their applications in mimicking the TME. In this regard, tissue engineering techniques are introduced to design more advanced and pathologically representative 3D in vitro models for studying the complexity of native TME and predicting clinical responses to anticancer therapeutics.

TME is a highly complex system comprising various functional components. An engineered system should enable precise spatiotemporal control of biophysical and biochemical factors such as stiffness change of extracellular matrix (ECM), interstitial fluid pressure, chemotaxis, and oxygen gradient. It should also include multiple cell types to mimic the tissue organization and cell–cell interactions. Both aspects are meaningful in tumor angiogenesis, cancer metastasis, and drug testing. Importantly, due to the remarkable advantages of engineering control, design versatility, and small sample consumption, microfluidic platforms are more suitable for establishing patient-derived personalized models than other approaches, which also offer the possibility to mimic the physiological flow via precise control of fluid flow speed and direction, or by incorporation of perfusable vasculature. On the other hand, engineering techniques can design a system that integrates spheroids or organoids into

microfluidic devices to meet the need for high-throughput drug screening.

Several previous reviews have focused on the development of spheroids,^[12] organoids,^[13] and tumor-on-a-chip,^[11,14] respectively. However, there is a lack of systematic and comprehensive evaluation of these three kinds of tumor models, especially on the inclusion of ECM in cancer modeling. Here, we outline the latest development of three types of advanced 3D tumor models in vitro, including spheroids, organoids, and tumor-on-chips, from a biomedical engineering perspective (**Figure 1**). We start with a brief overview of the components of TME and their roles in tumor progression. Subsequently, we describe how these engineering models can be used for modeling human cancer initiation, progression, and responses to therapies. Finally, we discuss the challenges and future perspectives in establishing 3D cancer models for industrial and clinical applications.

2. Overview of TME

TME is a complex and continuously evolving system comprising cellular components (heterogeneous cancer cells, endothelial cells, fibroblasts, mesenchymal stem cells, immune cells, etc.) and noncellular components (the supporting ECM, soluble factors, interstitial pressure, hypoxia, etc.) (**Figure 2**). TME not merely plays a critical role in tumorigenesis, progression, and metastasis but also significantly affects therapeutic efficacy. For example, environment-mediated drug resistance is a consequence of continuous interactions between cancer cells and their neighboring environment. As such, it is crucial to create 3D in vitro models for better capturing the complex TME with dynamic interactions between tumors and their surrounding stroma.

2.1. Cellular Components

2.1.1. Vascular Endothelial Cells

Vasculature lined with endothelial cells is essential for cancer growth and metastasis.^[15] To facilitate the supply of oxygen and nutrients, cancer cells, along with stromal cells within the TME, secrete various growth factors (e.g., vascular endothelial growth factor (VEGF), platelet-derived growth factors (PDGFs), fibroblast growth factor (FGF), etc.) to stimulate the formation of new blood vessels from the existing vasculature. This phenomenon is called angiogenesis and is considered a hallmark of cancer. With the help of the newly formed vessels, tumors could grow over 2–3 mm in diameter.^[16] However, compared with normal vasculature, tumor vasculature exhibits abnormal morphological and functional properties, such as disorganized vascular networks, leakiness, and heterogeneous blood flow. Such variations in vascular networks lead to increased interstitial fluid pressure (IFP) and areas of hypoxia, which in turn facilitate tumor survival and metastasis.^[16–17] In addition, the aberrant vasculature also restricts the access of recruited immune cells and anticancer therapeutics to tumors, resulting in reduced outcomes of cancer treatments.^[18] Thereby, considering vasculature is very necessary to mimic the TME in vitro.

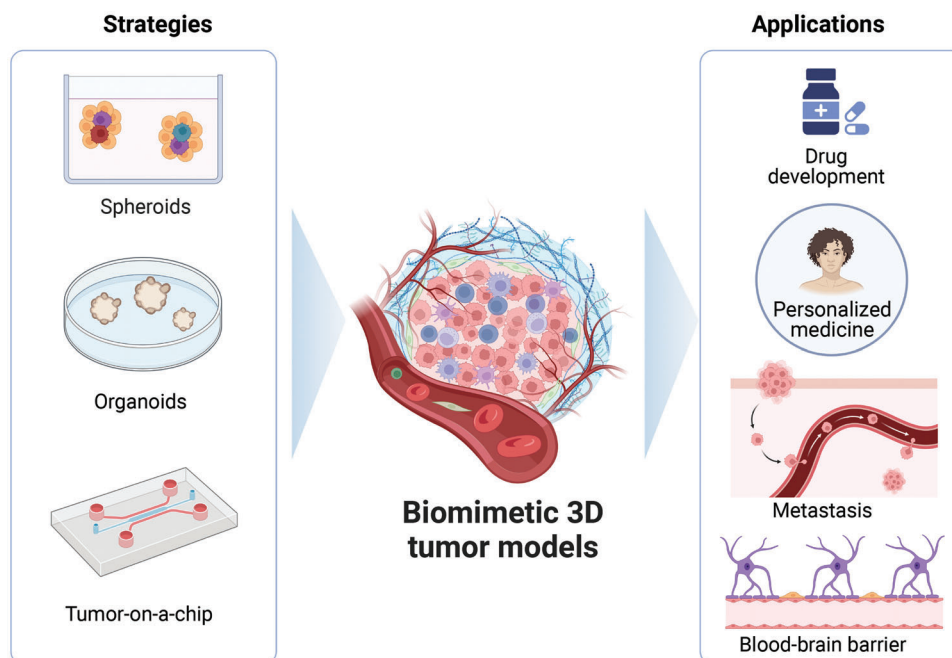


Figure 1. Schematic overview showing the in vitro strategies to simulate human TME in a 3D manner, including spheroids, organoids, and tumor-on-a-chip, and their applications in basic cancer research, clinical use, and drug development. Created with BioRender.com.

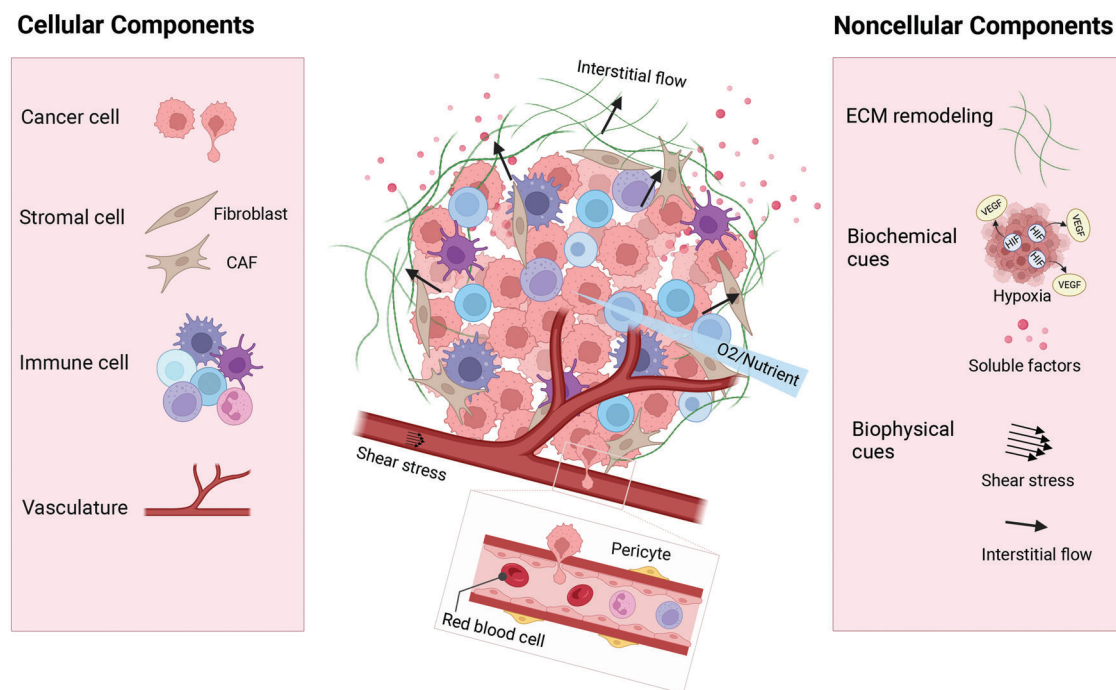


Figure 2. Schematic illustration of key components of the TME. TME is a highly complex system comprising cellular components and noncellular components, playing a critical role in cancer progression and evaluating therapy efficacy. Cellular components include heterogeneous cancer cells, stromal cells (e.g., fibroblast, cancer-associated fibroblast, etc.), endothelial cells, and diverse immune cells (macrophage, neutrophil, dendritic cell, etc.). Noncellular components include extracellular matrix, biochemical cues, and biophysical cues. Created with BioRender.com.

2.1.2. Cancer-Associated Fibroblasts

Cancer-associated fibroblasts (CAFs) are the most abundant cell types within the TME and are identified as large spindle-like stromal cells expressing α -smooth muscle actin, a phenotypic marker of activated fibroblasts. Lineage tracing studies in mice found that the origins of CAFs are highly heterogeneous. Most CAFs arise from normal local fibroblasts recruited and activated by cancer-secreted growth factors and cytokines in the TME.^[19] CAFs may also originate from bone marrow-derived mesenchymal stem cells,^[20] epithelial-mesenchymal transition (EMT) of epithelial cells,^[21] and endothelial cells that undergo endothelial-to-mesenchymal transition.^[22] However, these origins remain controversial. For example, the origin of CAFs from cholangiocyte EMT has been ruled out in cholangiocarcinoma.^[23]

CAFs contribute to tumor progression in multiple aspects. It has been shown that the high number of CAFs dwelling in the stroma correlates with poor clinical outcomes among patients with lung, breast, and pancreatic cancer.^[19,24] Once activated, CAFs start to produce abundant paracrine molecules, including transforming growth factor β 1 (TGF- β 1), stromal cell-derived factor-1 (SDF-1), hepatocyte growth factor (HGF), epidermal growth factor (EGF), PDGF, and VEGF. These molecules promote cancer growth, angiogenesis, and drug resistance. Despite the overwhelming evidence that CAFs are tumor-promoting, recent studies have suggested that CAFs might also serve as a negative regulator in cancer progression.^[25] On the other hand, CAFs can also secrete ECM components and release various proteolytic enzymes to remodel ECM, which can shape the TME to become more permissive to cancer growth and invasion.

2.1.3. Immune Cells

Generally, the immune cells within TME can be categorized into two main types: tumor-supporting and tumor-suppressive immune cells. Tumor-supporting immune cells mainly include M2-polarized macrophages, myeloid-derived suppressor cells, and regulatory T cells. In contrast, tumor-suppressive immune cells contain natural killer cells, effector T cells, M1-polarized macrophages, dendritic cells, and N1-polarized neutrophils. Both immune cells can shape the tumor behaviors and mediate therapy efficacy through direct contact or paracrine signaling. Among them, tumor-associated macrophages (TAMs) originating from circulating monocytes are the most abundant immune cells and are considered critical regulators of therapeutic response in the TME.^[26] Therefore, we mainly focus on the categories and functions of TAMs below. TAMs are generally classified into classically activated macrophages (M1) and alternatively activated macrophages (M2) according to their polarization status.^[27] M1-polarized macrophages are activated by exposure to Th1 cytokine interferon γ and microbial products. They are considered to suppress cancer growth through the secretion of pro-inflammatory cytokines.

In contrast, M2 macrophages differentiate in the presence of cytokines, such as IL-4, IL-10, IL-13, or TGF- β , and generally promote tumorigenesis through anti-inflammatory cytokines. M2 subsets can also facilitate angiogenesis and matrix remodeling during cancer development. Furthermore, high infiltration of M2

macrophages in tumor tissues is associated with poor clinical prognosis.^[28] Given the tumor-supporting role of TAMs, there is significant interest in reprogramming TAMs from tumor-promoting to tumor-suppressing cells.^[29]

2.2. Extracellular Components

2.2.1. Extracellular Matrix

The composition and microarchitecture of ECM vary depending on cancer type and stage of progression.^[30] ECM is a 3D protein network involving collagen, fibronectin, laminin, and glycosaminoglycans, which account for up to 60% of the TME.^[31] In tumor tissues, the ECM offers a mechanical supporting scaffold and cell-adhesive proteins for cellular components and serves as a reservoir for growth factors essential to cancer growth, invasion, and metastasis.^[32] During cancer development, tumor cells and tumor-associated stromal cells continuously change the composition and organization of ECM through deposition/degradation cycles and extensive crosslinking, shaping it more supportive for tumor growth.^[33] The increased deposition/crosslinking of ECM leads to a higher stiffness in the tumor-associated stroma than in normal tissues, promoting tumor invasiveness, and angiogenesis. In addition, the remodeled ECM synergizes with cell-cell crosstalk and the ECM architecture to pose a physical barrier to the penetration of immune cells, drugs, and antibodies to tumor sites. For example, Grantab et al. revealed that tumors with aligned collagen networks have lower drug penetration.^[34] Therefore, it is extremely important to reproduce the biochemical and biophysical properties of ECM when engineering 3D models in vitro.

2.2.2. Hypoxic Niche

Hypoxia, a hallmark of TME,^[35] presents in nearly all cancers. It is defined as a region with less than 2% oxygen levels, which arises from an imbalance between the rapid growth of tumor cells and the unmatched blood oxygen supply. The presence of hypoxia could trigger a variety of biological alterations in cancer cells, including altered gene expression and metabolic changes. As a result, cancer cells become more aggressive and resistant to chemotherapeutics.^[36] On the other hand, hypoxia also results in the enrichment of cancer stem cells.^[37] The aforementioned hypoxia-driven effects are related to the upregulation of hypoxia-inducible factors (HIFs). HIF proteins will rapidly accumulate in response to hypoxia as they cannot be degraded by the von-Hippel-Lindau tumor suppressor protein under hypoxic conditions. As HIF-1 has been recognized to be a key regulator of the response of mammalian cells to hypoxia, HIF-1-targeting therapies have attracted extensive attention in recent years.^[38]

2.2.3. Interstitial Fluid Pressure

Interstitial flow is a fluid flow through the stroma of tissues. In tumors, abnormal tumor-associated angiogenesis leads to an

increased influx of fluids into the tumor. However, the lymphatic system cannot efficiently drain out the increased influx of these fluids. This imbalanced flow results in a net interstitial fluid pressure (IFP) between the tumor mass and the surrounding stroma, which could increase to 30 mmHg at the tumor center.^[39] Besides vessel abnormalities, fibrosis, and contraction of the interstitial matrix may also involve increased tumor IFP. The elevated IFP in tumors forms a barrier to anticancer drug delivery, which is an obstacle in cancer treatment.^[40] Recently, high IFP in the tumor was found to have a good correlation with poor clinical outcomes.^[41] In addition, the interstitial flow was also demonstrated to promote angiogenic and lymphatic sprouting.^[42] Therefore, decreasing the tumor IFP is considered an attractive approach to improving drug uptake and efficacy.

3. Strategies for Physiologically Relevant 3D Models

This section illustrates different engineered approaches to reconstituting the TME, including spheroids, organoids, and tumor-on-a-chip. The characteristics, fabrication methods, and applications of each strategy are reviewed. Meanwhile, combining these approaches for better emulating the TME complexity is highlighted, which could largely help reveal the mechanism of cancer progression and develop new anticancer drugs.

3.1. Spheroids

3D tumor spheroids are micro-sized cancer cell aggregates formed by 3D cell culture *in vitro*, which can be categorized as homotypic spheroids (monoculture) and heterotypic spheroids (coculture of tumor cells and stromal cells).^[43] If grown larger than 400 μm , these tumor spheroids can generate *in vivo*-like oxygen and nutrient gradients with a necrotic core, a quiescent intermediate region, and a thick proliferating outer shell due to limited molecular transport, which create unique opportunities for studying the impact of hypoxia on tumorigenesis, angiogenesis, and drug efficacy.^[44] In addition, spheroids can also replicate cell–cell interactions,^[45] growth kinetics,^[46] and *de novo* ECM deposition of solid human tumors.^[47] Furthermore, growing evidence showed that the strong cell–cell contacts of tumor spheroids in combination with dense ECM deposition is responsible for chemoresistance by posing a physical barrier to the penetration of chemotherapeutics and immune cells similar to *in vivo*.^[48] Given their tumor-like properties, tumor spheroids have been used as routine drug screening models to reduce drug development costs and unnecessary animal experiments.^[49]

Nowadays, 3D tumor spheroid production approaches can be categorized into two main types: scaffold-free or scaffold-based approaches. Each method possesses certain advantages and disadvantages, as summarized in **Table 1**. More detailed descriptions of the principle and features of these techniques can be found in the previous reviews.^[50] An important point to consider is spheroid size and heterogeneity may influence the robustness of endpoint assays, so the choice of the production method relies on the application desired.

3.1.1. Scaffold-Free Approaches

Scaffold-free methods typically include spinner flasks, magnetic levitation, hanging drop technique, and ultralow attachment plates.^[51] Generally, these methods promote cell–cell interactions by inhibiting cell–substrate interactions, thus rapidly facilitating cells to self-assemble into multicellular aggregates. Scaffold-free methods are relatively simple and able to obtain high-throughput capabilities with the flexibility to combine multiple cell types.^[52] They have thereby been utilized in spheroid culture for fundamental biology studies and drug screening.

Recently, liquid marbles coated with hydrophobic silica particles^[53] were developed to culture tumor spheroids for drug screening. They allow real-time *in situ* imaging and motility control compared to conventional hanging drops. However, these well-established and routine methods are based on the macroscale culture systems. They require large consumption of cells and compounds, hindering their applications in the screening of rare cell-derived spheroids, such as patient tumor biopsy samples. To address this limitation, Popova et al. presented a miniaturized droplet microarray based on hydrophilic–superhydrophobic patterning for fast and high-throughput production of tumor spheroids in nanoliter droplets.^[54] Due to their robust experimental process and precise control of spheroid size, this system could be exploited with high-throughput screening (HTS) platforms for drug screening. For example, tumor spheroids derived from five colorectal cancer patients were formed within 36 h for testing the efficacy of three common chemotherapeutics (5-fluorouracil, cetuximab, and panitumumab).^[55] It was demonstrated that these tumor spheroids could resemble *in vivo* drug response, suggesting the potential use of this platform in precision medicine.

As another highly miniaturized culture method, microwell arrays are developed to generate spheroids with well-defined sizes and shapes. In general, microwell arrays are engineered into a concave shape with a nonadherent surface (e.g., poly(2-hydroxyethyl-methacrylate), agarose coatings, etc.) so that cells sediment to the bottom of microwells by gravity and thereby generate spheroids via close cell–cell interactions. One example was the fabrication of a polydimethylsiloxane (PDMS)-based microwell array with tapered bottom by soft lithography to efficiently culture patient-derived circulating tumor cell (CTC) clusters.^[56] It was shown that the custom tapered microwells allowed the robust formation of CTC clusters without pre-enrichment and rapid drug sensitivity feedback within two weeks, overcoming the deficiency of conventional cylindrical microwells, with automated readouts facilitating routine screening for clinical utility.^[57]

Similarly, Jiang and colleagues designed a PDMS-based microwell array with conical bottom by 3D printing for MDA-MB-231 breast cancer spheroid culture (**Figure 3a**).^[58] In this study, the tumor spheroids formed in microwells displayed comparable viability to those in 2D cultures, indicating that microwells offer a suitable environment for spheroid culture. By coculture of tumor spheroids with Jurkat T cells, this system allowed for high-throughput assessing immune checkpoint inhibitor-based therapy. Despite their ease of use, PDMS-based microwells suffer from nonspecific absorption of compounds and fail

Table 1. Advantages and disadvantages of different techniques used for tumor spheroid production.

Methods	Advantages	Disadvantages
Spinner flasks	<ul style="list-style-type: none"> • Simple to use • Easy to set up • Mass production of tumor spheroids • Long-term culture 	<ul style="list-style-type: none"> • Poor control of spheroid morphology and size • High shear stress • High variability in size • Need transfer spheroids for downstream analysis
Hanging drop	<ul style="list-style-type: none"> • Simple to use • Easy to set up • Low shear stress • Good size/shape control • Compatible with standard liquid handling robotics 	<ul style="list-style-type: none"> • Labor intensive • Difficult to produce large spheroids and change medium • Short-term culture • Not compatible with in situ imaging
Magnetic levitation	<ul style="list-style-type: none"> • Enable in situ imaging and analysis 	<ul style="list-style-type: none"> • A limited number of spheroids can be generated • Cells require to be pretreated with magnetic beads • High concentration of beads may be toxic to cells
Ultra-low attachment plates	<ul style="list-style-type: none"> • Large number of spheroids can be produced • Can be multiplexed with imaging and other biochemical assays • Long-term culture 	<ul style="list-style-type: none"> • Poor size/shape homogeneity • Needs plate-coating procedure
Microwells	<ul style="list-style-type: none"> • Good size/shape control • High throughput/reproducibility • Reduced medium consumption • Allows the incorporation of mechanical properties 	<ul style="list-style-type: none"> • Involves lithographic or printing processes • Difficult to maintain microwell integrity
Macroscopic 3D matrix	<ul style="list-style-type: none"> • High throughput • Allows the incorporation of mechanical properties 	<ul style="list-style-type: none"> • Difficult to retrieve cells without damage • Poor size/shape homogeneity
Microgels	<ul style="list-style-type: none"> • Precise control over size/shape • High throughput • Small sample consumption • Allows the incorporation of mechanical properties 	<ul style="list-style-type: none"> • Limited biomaterials available • Fabrication process may decrease cell viability
3D bioprinting	<ul style="list-style-type: none"> • Enable spatial control of biomaterials and cell components • Easy to scale up • Can be multiplexed with imaging and other biochemical assays • Compatible with microfluidic devices 	<ul style="list-style-type: none"> • Needs to optimize the bioinks • Printing process may decrease cell viability

to provide a broad spectrum of biochemical and mechanical properties for spheroid growth. To address these challenges, the microwells are subsequently fabricated from micropatterning hydrogels such as agarose^[59] and methacrylated gelatin (GelMA).^[60] In one study, Luan et al. produced lung tumor spheroids with uniform size and high viability using U-shaped agarose microwells.^[61] Spheroids from three lung cancer cell lines (H1975, A549, HCC4006) were used to screen two epidermal growth factor receptor tyrosine kinase inhibitors (gefitinib and osimertinib), and the therapeutic efficacy exhibited clinical relevance. They also demonstrated the ability of their platform to culture patient-derived spheroids. The produced spheroids had high viability of $89\% \pm 7.1\%$ even after being cultured for 7 days, highlighting their potential for application in patient-derived organoid culture. To mimic the native TME, hydrogel-based microwells with tunable components and stiffness were developed to efficiently generate HCC1806 multicellular structures (Figure 3b).^[60a] Two distinct hydrogels, polyethylene glycol diacrylate (PEGDA) and methacrylated gelatin (GelMA), were utilized to microfabricate the microwells. They found that HCC1806

cells formed larger spheroids in GelMA microwells than in PEG microwells, and high stiffness caused a significant difference in spheroid proliferation/metabolic activity, suggesting the effect of tumor-ECM crosstalk on cancer spheroid size. Another merit of hydrogel-based microwells is that stromal cells or additional ECM components can be incorporated into the system. A follow-up study from the same group presented a stromal cell-laden hydrogel-based microwell system with low or high stiffness, mimicking normal and tumor-associated stroma, where the crosstalk of tumor spheroids with stromal cells highly depended on ECM stiffness.^[60b] Although 3D tumor spheroids prepared from scaffold-free approaches have been widely employed for HTS owing to similar drug response and gene expression to that of in vivo solid tumors,^[6b] they are intrinsically limited in the lack of pre-existing ECM during spheroids assembly. Emerging evidence has demonstrated that the inclusion of spheroids within ECM contributes to better reproducing of tumor-specific hallmarks.^[62] Therefore, scaffold-based platforms may present alternative approaches to generating more physiologic tumor spheroids.

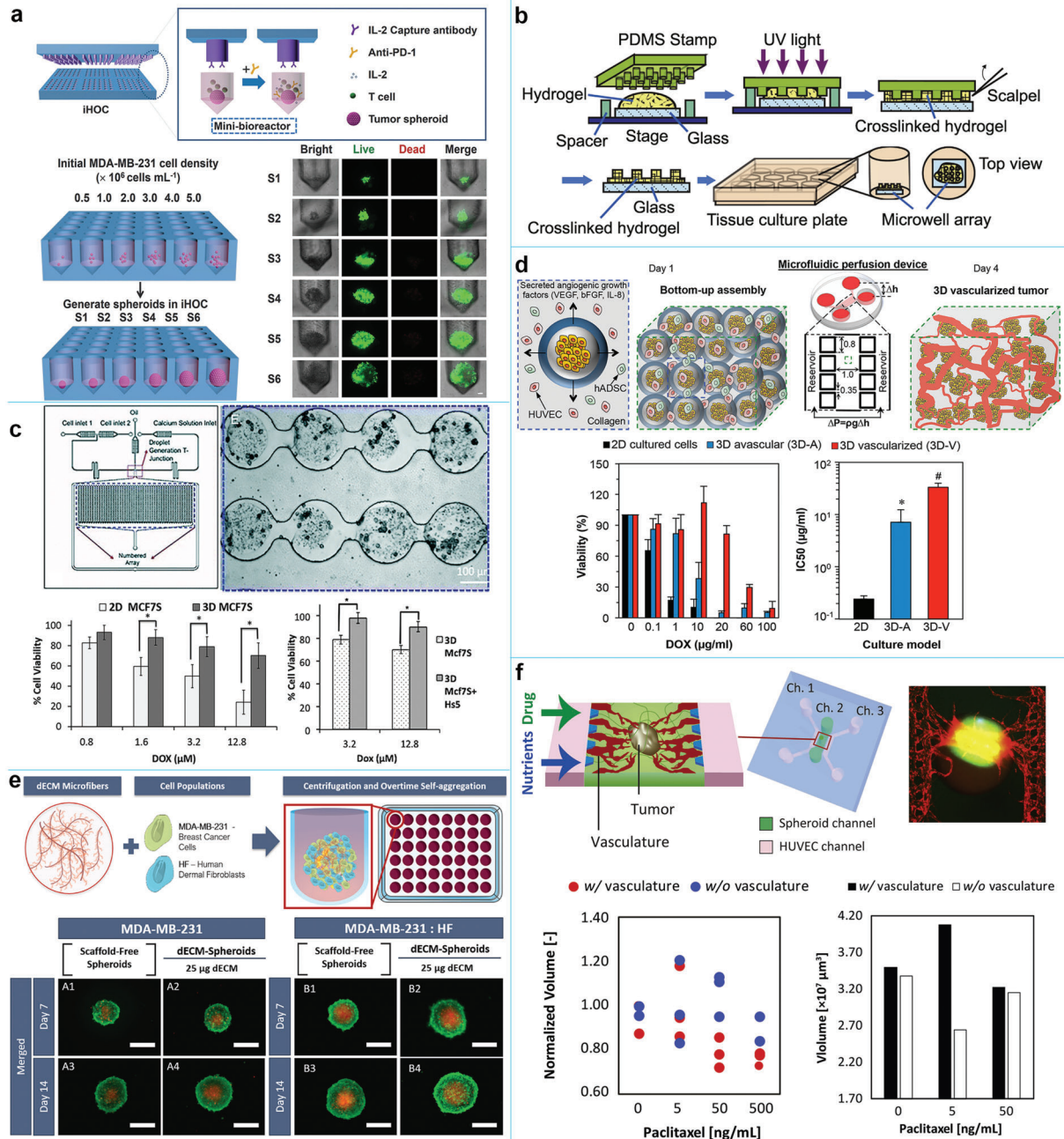


Figure 3. Spheroid models. a) PDMS-based microwell arrays for culturing tumor spheroids to monitor the interactions among tumor spheroids, immune cells, and immune checkpoint inhibitors. Reproduced with permission.^[58] Copyright 2021, Wiley-VCH GmbH. b) Schematic illustration of the fabrication of hydrogel-based microwell arrays for studying the effect of substrate composition and stiffness on tumor formation. Reproduced with permission.^[60a] Copyright 2017, IOP Publishing. c) Spheroids generated in a droplet-based microfluidic platform for drug-based cytotoxicity screening ($p < 0.05$). Reproduced with permission.^[67] Copyright 2016, Royal Society of Chemistry. d) Hybrid hydrogel of collagen and alginate for fabrication of tumor spheroids for drug screening. Reproduced with permission.^[72] Copyright 2017, American Chemical Society. e) Decellularized matrix for preparation of tumor spheroids for high-throughput drug screening. Scalebars = 400 μm . Reproduced with permission.^[78] Copyright 2021, Elsevier. f) Spheroids-on-a-chip for studying the role of vascular perfusion in drug efficacy. Reproduced with permission.^[81] Copyright 2020, Elsevier.

3.1.2. Scaffold-Based Approaches

In scaffold-based approaches, tumor cells proliferate in/on a tumor ECM-mimetic matrix. Such scaffolds not only support cell growth but also provide the in vivo-like biophysical and

biochemical cues that are essential to regulate tumor cell functions.^[63] To date, the scaffolds for in vitro cancer modeling have been engineered from natural hydrogels (e.g., proteins, polysaccharides), synthetic hydrogels (e.g., PEG, peptides, etc.), and their hybrids given their high water content, tissue-like

bioactivity, viscoelasticity, and mechanical properties. In recent years, the advances in microfabrication technologies have enabled the generation of more accurate and sophisticated hydrogel-based platforms that capture key features of the TME compared to standard macroscopic 3D hydrogels. These include microgel-based and 3D bioprinting-based platforms. Their advantages and drawbacks are shown in Table 1.

Currently, various tumor spheroids have been fabricated by embedding cancer cells into protein-based hydrogels such as Matrigel,^[64] fibrin,^[65] and collagen^[66] as they incorporate specific cell-adhesive motifs and enzymatic-mediated matrix degradation which are beneficial to cell proliferation. Nonetheless, high batch-to-batch variability and poor mechanical properties remain the bottlenecks of such hydrogels for tumor spheroid culture. To address these issues, polysaccharides and synthetic hydrogels with beneficial mechanical properties are extensively utilized to generate 3D tumor spheroids, such as alginate, hyaluronic acid, chitosan, etc. For instance, Sabhachandani et al. generated breast cancer monoculture and coculture spheroids in cell-laden alginate microgels via droplet-based microfluidic platforms and explored their potential in therapeutic efficiency screening (Figure 3c).^[67] Their results showed that monoculture and coculture spheroids displayed higher drug resistance than 2D monolayers. To more closely recapitulate the native TME, further studies from the same group also incorporated an oxygen gradient generator and immune cells into their spheroid systems to study the role of hypoxia and immune cells in spheroid growth and drug response, respectively.^[68] Recent groups have also explored the implications of immune cells on tumor response and progression.^[69]

Although natural polysaccharides recapitulate structural aspects of the ECM, batch variability still limits their extensive use in cancer modeling. As such, considerable efforts have been focused on developing synthetic hydrogels, such as PEG and peptides, in the culture of tumor spheroids due to their high reproducibility as well as controllable and stable mechanical properties. Loessner et al. synthesized a PEG-based hydrogel functionalized with integrin ligands and matrix metalloproteinase (MMP)-sensitive sites to culture tumor spheroids.^[70] The authors demonstrated that OV-MZ-6 and SKOV-3 ovarian cancer cells generated compact spheroids within these synthetic hydrogels. Moreover, the inclusion of arginine-glycine-aspartate peptides in such hydrogels significantly enhanced the proliferation of spheroids, indicating that integrin activation plays a critical role in tumor spheroid growth. Studies on drug testing showed that ovarian cancer cell spheroids were more resistant to paclitaxel treatment than 2D culture, highlighting the potential of spheroid culture in mimicking *in vivo*-like chemoresistance. To mimic the nanofibrous network of native ECM, peptide-based self-assembling hydrogels were designed to incorporate relevant proteins of the ovarian TME for ovarian tumor spheroid culture.^[71] The results demonstrated that the self-assembling platforms enabled modeling the TME of ovarian cancer to a comparable level, yet more controlled than that offered by Matrigel. However, such hydrogels require additional modifications with cell adhesion moieties and MMP degradable sites, and the preparation and purification procedures are labor- and cost-intensive. Therefore, a combination of natural proteins with synthetic polymers or polysaccharides is a simple yet effective method for offer-

ing cell adhesion ligands as well as tunable mechanical properties of the hydrogel, which facilitate spheroid growth. For example, composite collagen-alginate microcapsules laden with breast cancer cells (MCF-7) were reported to create 3D vascularized tumor spheroids by suspending these core-shell microbeads inside an external stromal cell-laden collagen matrix (Figure 3d).^[72] The microcapsules were assembled with the surrounding endothelial cells and human adipose-derived stem cells, allowing for direct observation of vasculature formation and further use of the system in the drug efficacy evaluation. Moreover, the cells cultured in this system showed higher *in vivo* tumorigenicity than in 2D culture.

In addition, hybrid hydrogels have been commonly used as bioinks to fabricate scaffolds for tumor spheroid culture since 3D bioprinting emerged. Due to its precision in the spatial control of cells and biomaterials within complex 3D architectures, the 3D bioprinting technique enables construction of biomimetic models with functional complexity, well-defined components, and tunable mechanical properties.^[73] In addition, its capability of rapid prototyping also provides an opportunity for the mass production of 3D tumor spheroids. As an example, colorectal cancer spheroids were formed by high-throughput bioprinting into 96-well plates, which allowed scalable spheroid culture and automated imaging with high-content microscopes.^[74] Tumor spheroids from freshly isolated human intrahepatic cholangiocarcinoma biopsy samples were also prepared by this platform, indicating its potential in the development of personalized tumor models.^[75]

Polysaccharide and synthetic hydrogels also allow for flexibly changing their mechanical properties by controlling hydrogel concentration, crosslinking density, and crosslinking manner, which facilitates the study of the role of hydrogel stiffness in growth, invasion, and drug resistance of tumor spheroids. For example, a fibrillar alginate-collagen hydrogel was used to evaluate how stiffness affected the growth of MCF-7 cancer spheroids without a noticeable change in its pore size and fibrillar architecture. The results revealed that MCF-7 tumor spheroids in soft hydrogels grew larger and displayed higher resistance to doxorubicin.^[76] In another study, tumor spheroids grown in soft hydrogels demonstrated increased invasiveness *in vitro* and high tumorigenicity when implanted *in vivo*.^[77]

Recently, tissue-derived decellularized ECM (dECM) has been leveraged as a biomaterial for 3D spheroid assembly owing to its ability to emulate native tissue ECM faithfully. For instance, to replicate pre-existing ECM presence in the *in vivo* setting, Ferreira and co-workers reported using breast tissue-specific ECM isolated from porcine to culture tumor spheroids (Figure 3e). They found that the incorporation of decellularized microfibrillar fragments contributed to the spheroids exhibiting higher necrotic core formation compared with standard spheroids,^[78] highlighting the importance of ECM in recapitulating this hallmark of native tumors. Moreover, the dECM-enriched heterotypic spheroids captured the *in vivo* invasive profile and exometabolomic signatures. In a different approach, liver tumor spheroids were generated from 3D printed liver dECM-based scaffolds with tunable mechanical properties, facilitating the study of how the clinically relevant 3D matrix stiffness affecting hepatocellular carcinoma progression.^[79] The authors observed that HepG2 cells demonstrated a smaller spheroid size

and increased invasion potential in stiff scaffolds compared to those in soft scaffolds.

With the advances in microfluidic technologies, spheroids-on-chip models have achieved growing interest in studying the role of blood flow in the growth and drug delivery of tumor spheroids.^[72,80] Nashimoto et al. incorporated tumor spheroids with perfusable vascular networks to assess the tumor activities under intraluminal flow.^[81] In this model, the perfusion via the engineered vascular networks could be maintained for more than 24 h (Figure 3f), which markedly enhanced the proliferation activities of tumor spheroids. Interestingly, the dose-dependent effect of antitumor drugs on tumor activities was not observed under perfusion conditions in contrast to static conditions, highlighting the significance of recapitulating vascular flow in assessing tumor activities in drug screening.

3.2. Organoids

Although tumor spheroids from cell lines have been widely explored to investigate cancer growth, invasion, and drug screening, they fail to replicate the complex biological and clinical features of primary tumor tissues, limiting their use in precisely predicting patient-specific responses to chemotherapeutic agents. To overcome this limitation, organoids have emerged as excellent tools in disease modeling, drug screening, and the development of personalized medicine. Unlike spheroids, tumor organoids are self-organizing, 3D multicellular structures generated from primary patient samples in a 3D matrix.^[82] Most importantly, tumor organoids preserve critical structural and functional features of their *in vivo* counterparts,^[82] which may provide a correlative *in vitro* platform with unprecedented predictiveness for clinical decision-making. Thus, this versatile technology has been considered as the next-generation tumor surrogate and has contributed to the development of various new human tumor models, including lung,^[83] breast,^[84] pancreatic,^[85] colorectal,^[86] ovarian,^[87] prostate,^[88] and stomach cancer.^[89]

Unlike spheroid cultures that have adopted a variety of biomaterials, tumor organoids were conventionally generated in animal-derived proteinaceous ECM gels, most prominently the basement membrane extract (BME) Matrigel, which is a “gold standard” hydrogel for 3D culture. By embedded in commercially available Matrigel, organoids derived from gastrointestinal tumor have been presented by Vlachogiannis et al.^[90] In this paper, the patient-derived organoids (PDOs) exhibited a high degree of similarity to the original patient tumors in phenotype and genotype. Further drug testing revealed that these PDOs could capture patient responses in the clinic. However, current organoid culture protocols are nonstandardized and ill-defined across cancer types. To address this issue, Larsen et al. recently developed a robust pan-cancer organoid platform with chemically defined minimal media, which supported tumor organoid culture from over 1000 patients.^[91] Apart from bulk matrix encapsulation, droplet emulsion microfluidics (e.g., microgels)^[92] and 3D bioprinting^[93] are also applied to fabricate Matrigel-based PDOs, which are similar to the scaffold-based approaches for spheroid generation. These two platforms both allowed for rapid PDO generation (< 2 weeks) in high throughput as well as compatibility

with automation dispensers, facilitating their application in personalized drug screening.

Matrigel is a mouse tumor BME comprising laminin, collagen IV, and proteoglycans, as well as nidogen and growth factors.^[84–87] Although it has exhibited to be suitable for supporting organoid culture, the ill-defined composition, immunogenicity, and batch-to-batch variability in Matrigel resulted in its reduced reliability as a matrix for PDO culture.^[84,87–89] Additionally, the mechanical properties of BME cannot be tailored, rendering it unable to study mechanotransduction during organogenesis.^[64,65] Thus, there is a strong need to develop alternative biomimetic hydrogels in the use of organoid cultures.

Several biomimetic hydrogels, such as proteins, polysaccharides, and synthetic hydrogels, have been to date developed as alternative matrices for organoid growth. For example, Ng et al. fabricated enzymatically crosslinked gelatin with independent tuning stiffness and composition to grow patient-derived xenograft colorectal cancer organoids (Figure 4a).^[94] They demonstrated that these gelatin-based hydrogels could support colorectal cancer organoid growth and metabolism comparably to those cultured in Geltrex. In another study, a fully synthetic PEG-based hydrogel was designed for cancerous pancreatic organoid growth.^[95] This microenvironment-inspired matrix was fabricated by eight-arm PEG, MMP-sensitive crosslinker, and three adhesion-mimetic peptides. The authors found that the organoids matured and developed on this artificial hydrogel with similar growth and architecture as on Matrigel. Aiming to emulate the filamentous architecture of the breast cancer ECM, a nanofibrillar hydrogel consisting of cellulose nanocrystals and gelatin (EKGel) was proposed.^[96] This hybrid hydrogel could initiate and grow multiple breast cancer PDOs (Figure 4b). Interestingly, PDOs grown in this matrix exhibited similar growth, histopathologic features, gene expression, and drug response to *in vivo* and PDOs generated in BME. The results showed that EKGel had the potential to replace BME in the breast cancer PDO culture.

Another example is using hybrid collagen-hyaluronic acid hydrogels to support the growth of lung adenocarcinoma organoids.^[97] The authors found that the organoids grown in this composite hydrogel maintained a similar phenotype to the *in vivo* scenario. Moreover, the *in vitro* organoids exhibited higher resistance to chemotherapeutic agents than that generated in conventional 2D culture, further indicating the significance of 3D cell culture and the incorporation of ECM-mimetic matrix. To improve tumor organoids correlation with the *in vivo* setting, tumor organoids were recently cocultured with patient-derived CAFs and immune cells.^[98] In addition, tissue-derived dECM hydrogels have also been extensively explored for culturing PDOs^[99] due to their biomimicry of native tissue ECM. Tienderen and colleagues exploited tumor tissue-derived dECM to culture cholangiocarcinoma organoids and found that the tumor ECM induced a transcriptome profile more closely resembling patient tumor tissue than BME or normal tissue ECM.^[100] Notably, hydrogel-based microwell arrays with a U shape were engineered by Lutolf group^[101] for high throughput generation of patient-derived colorectal cancer organoids as they are superior in standardization and reproducibility compared to the traditional 3D-culture

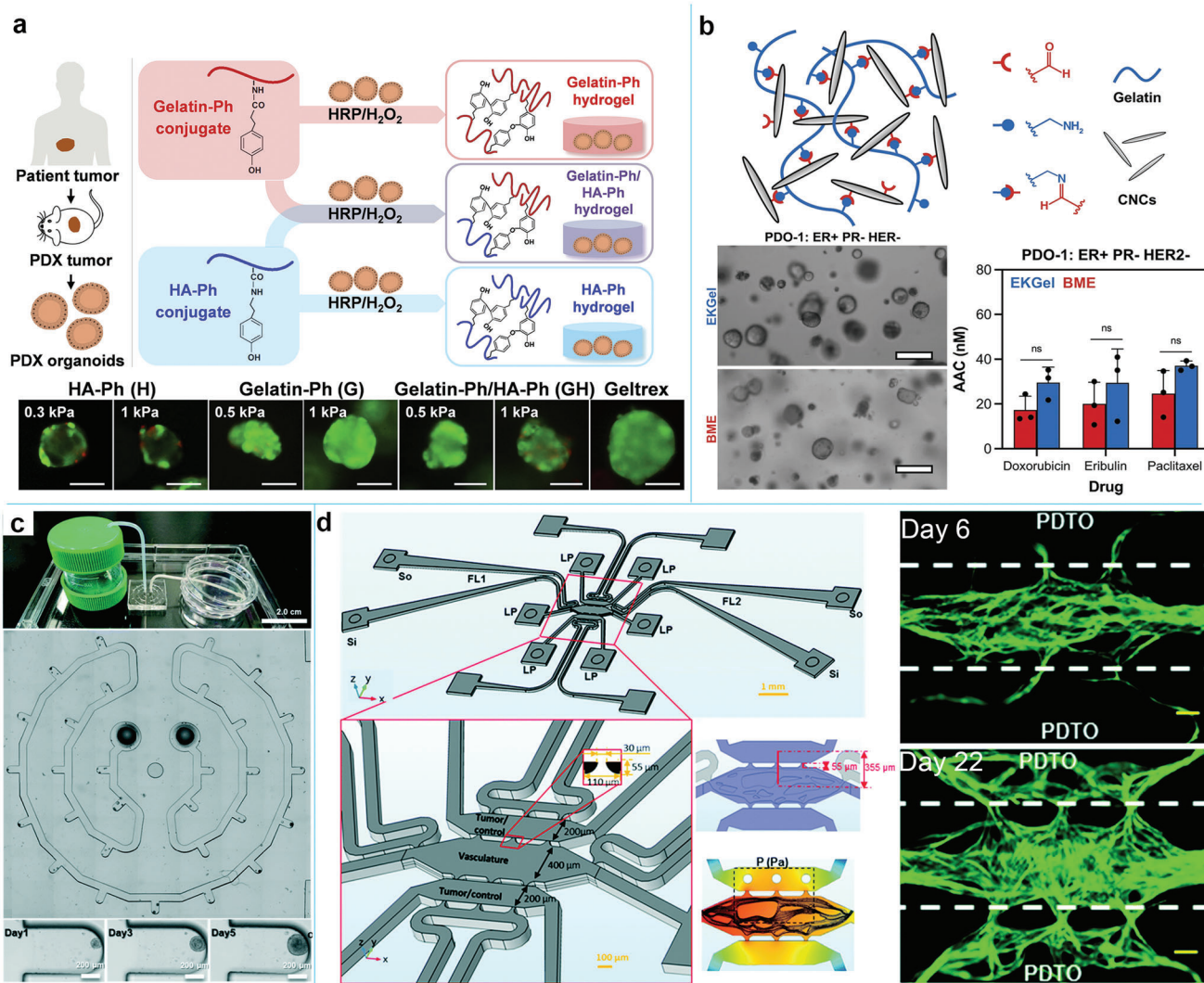


Figure 4. Organoid models. a) Schematic illustration of PDX-derived tumor organoid encapsulated in enzymatically crosslinked HA-Ph, gelatin-Ph, or gelatin-Ph/HA-Ph hybrid hydrogels with tunable stiffness. Scale bars: 100 μm. Reproduced with permission.^[94] Copyright 2019, Elsevier. b) Schematics of ECM-mimetic EKGel for growth of breast PDOs. Reproduced with permission.^[96] Copyright 2022, Springer Nature. c) Microfluidic-based organoid culture for drug sensitivity testing. Reproduced with permission.^[103] Copyright 2019, Royal Society of Chemistry. d) Vascularized organoids chips for mimicking physiological delivery of drug to tumor sites. Scale bars: 100 μm. Reproduced with permission.^[104] Copyright 2019, Royal Society of Chemistry.

setting. To confirm the potential of their approach in high-content phenotypic drug testing, 80 anticancer compounds were tested to determine their efficacy.

In static 3D culture, organoids rely on passive diffusion to exchange nutrients and wastes. Nonetheless, diffusive transport becomes insufficient when organoids grow larger to support their growth and maturation. In this context, organoids-on-a-chip platforms that combine microfluidic technology and organoids become a promising approach to overcoming these challenges due to their capacity to provide a dynamic supply of nutrients in a physiological flow.^[102] For instance, Jung et al. engineered a lung cancer organoids-on-a-chip platform consisting of 29 microwells and a flow microchannel that supports PDOs culture and drug sensitivity test under a continuous flow condition (Figure 4c).^[103] 3D lung cancer organoids formed in this platform re-

tained the morphological and genetic characteristics of the original patient tumor. They demonstrated higher sensitivity to cisplatin and etoposide than those under static culture conditions due to the increased drug penetration in the microfluidic platform. These results suggested that their platform offered a more physiologically relevant 3D TME to predict drug responses. In another study, to closely simulate the pathological flow environment of blood vessels, vascularized tumor organoids-on-a-chip was designed by Shirure et al. (Figure 4d).^[104] This model was created by coculture of tumor organoids with a perfused 3D microvascular network in a 5-channel microfluidic device, which allowed vascularization of tumoroids and their perfusion under in vivo-like physiological flow that captured transport features of the in vivo TME. Furthermore, the vascularization of tumoroids can be maintained for 22 days. By showing a dramatic reduction

of tumor proliferation after vascular perfusion with paclitaxel, this study also indicated the potential use of this model for assessing patient-specific responses to chemotherapy in clinical trials.

Additionally, these miniaturized versions of organs are highly suitable for high throughput screening preclinical drugs when combined with microfluidic chips. As demonstrated by Schuster and co-workers, an automated microfluidic platform incorporated with human-derived pancreatic tumor organoids was designed for dynamic personalized therapies.^[105] With the aid of a real-time imaging system, the researchers observed big differences in the responses of individual PDOs to specific drug treatments and found that dynamic drug treatment was more effective than constant-dose administration methods. More recently, by integrating a concentration gradient generator with microwell arrays of organoid culture, Prince et al.^[106] engineered a microfluidic platform that enabled both in situ culturing of large arrays of breast cancer PDOs within a biomimetic hydrogel and high-throughput screening anticancer drugs under dynamic flow conditions. It was found that drug sensitivity of breast cancer PDOs in this platform recapitulated in vivo drug sensitivity after perfusion for 5 days, suggesting the potential of this proposed platform to be used as an in vitro preclinical approach for developing personalized cancer therapies and effectively screening novel antitumor drugs. Importantly, due to small sample consumption, tumor chips show promise in culturing scarce cancer slices that retain the original TME relatively intact for multiplexed drug testing.^[107] As an example, cuboid-shaped microdissected glioma tissues with well-preserved native TME were trapped on a 3D-printed multiwell microfluidic platform for direct drug testing.^[108]

Although organoids replicate the structural and functional features of patient TME and are envisioned to be the next generation of 3D in vitro models for drug screening and basic cancer biology studies,^[109] human clinical trials on PDOs for drug screening are currently ongoing. To accelerate this process, some challenges still need to be addressed, including optimizing the culture conditions required for organoid generation, reducing the time and cost of organoid cultures, and incorporating stromal cells, especially immune cells, into organoids.

3.3. Tumor-on-a-Chip

Over the past decades, advances in microfluidic technology and tissue engineering have made hydrogel-based microfluidic platforms promising candidates to replace conventional experimental models in recapitulating some key features of the TME (e.g., the cancer metastasis cascade, dynamical blood flow, cell–cell and cell–ECM interactions) and accurately predicting patient responses. This is because microfluidic systems have the capability to accurately control multiple microenvironmental factors and incorporate distinct cell types in vitro. Importantly, microfluidic models only require a low number of cells, rendering them superior to patient biopsy samples. In this section, we will introduce the state-of-the-art applications of tumor chips in modeling cancer metastasis, therapeutic response, and blood–brain barrier (BBB) in brain cancer, mainly focusing on hydrogel-based microfluidic devices.

3.3.1. Microfluidic Modeling Metastatic Cascade

Metastasis is responsible for 90% of cancer-related deaths. However, the underlying cellular and molecular mechanisms that drive this process remain poorly understood. Most conventional models fail to replicate the highly complex metastasis process fully. Furthermore, recent studies have revealed that the number of CTCs in blood samples correlates with early recurrence and poor prognosis.^[110] As such, many microfluidic metastatic models have been engineered to dissect the cellular and molecular players in the tumor metastasis cascade, which is pivotal to deciphering new opportunities for therapeutic intervention during early metastatic dissemination.

Modeling Tumor Angiogenesis: Angiogenesis is a critical step in cancer progression as its initiation represents the progression from hyperplasia toward neoplasia^[111] and has become an essential factor in controlling cancer growth and progression. Multiple hydrogel-based microfluidic devices have been engineered to study the angiogenesis induction by tumor cells. Kim et al. cocultured human umbilical vein endothelial cells (HUVECs) with malignant human glioma cells (U87MG) in a fibrin-based microfluidic device with micropillar partitions (**Figure 5a**).^[112] It was observed that the endothelial cells invaded the adjacent matrix and generated angiogenic sprouts. Moreover, the sprouts fused with neighboring vessels rather than growing directionally toward the cancer cells, which corresponds to in vivo observations. Apart from mimicking the angiogenic sprouting from a 2D monolayer, artificial vessels with a 3D tubular structure are engineered by template-based micromolding for modeling tumor-induced angiogenesis. Such an example was reported by Miller et al. They modeled the crosstalk between endothelial cells (HUVECs) and primary patient cancer cells in a lumen-based microfluidic device where patient-derived renal cell carcinoma (RCC) tumor clusters were embedded in the matrix surrounding artificial blood vessels.^[113] The results showed that these primary tumor clusters significantly triggered the angiogenic sprouting of HUVECs.

On the other hand, angiogenic sprouting can also be induced by angiogenic stimulators (e.g., VEGF, HGF, β -FGF, etc.).^[114] The work by Nguyen and colleagues presented an organotypic microfluidic platform recapitulating angiogenic sprouting and new microvessel formation in vitro through artificial engineering vessels in a collagen matrix (**Figure 5b**).^[114c] Using this model, the authors observed that capillary sprouts invaded the surrounding matrix, eventually linking to functional neovessels after the perfusion of proangiogenic factors through the adjacent lumen. Additionally, tumor-associated angiogenesis is also affected by the interstitial flow. A multichannel microfluidic device containing endothelial cells and normal human lung fibroblasts was used to investigate the role of interstitial flow in angiogenesis. The results showed that angiogenic sprouting was facilitated only when the direction of flow and sprout was opposite. Furthermore, in the presence of proangiogenic factors, interstitial flow against the direction of sprouts significantly promoted the initiation and outgrowth of angiogenic sprouts.^[42a] Similar results were observed by studying the role of interstitial flow in lymphatic sprouting.^[42b]

Due to its ability to provide a physiologically relevant microenvironment, the microfluidic angiogenesis model has also

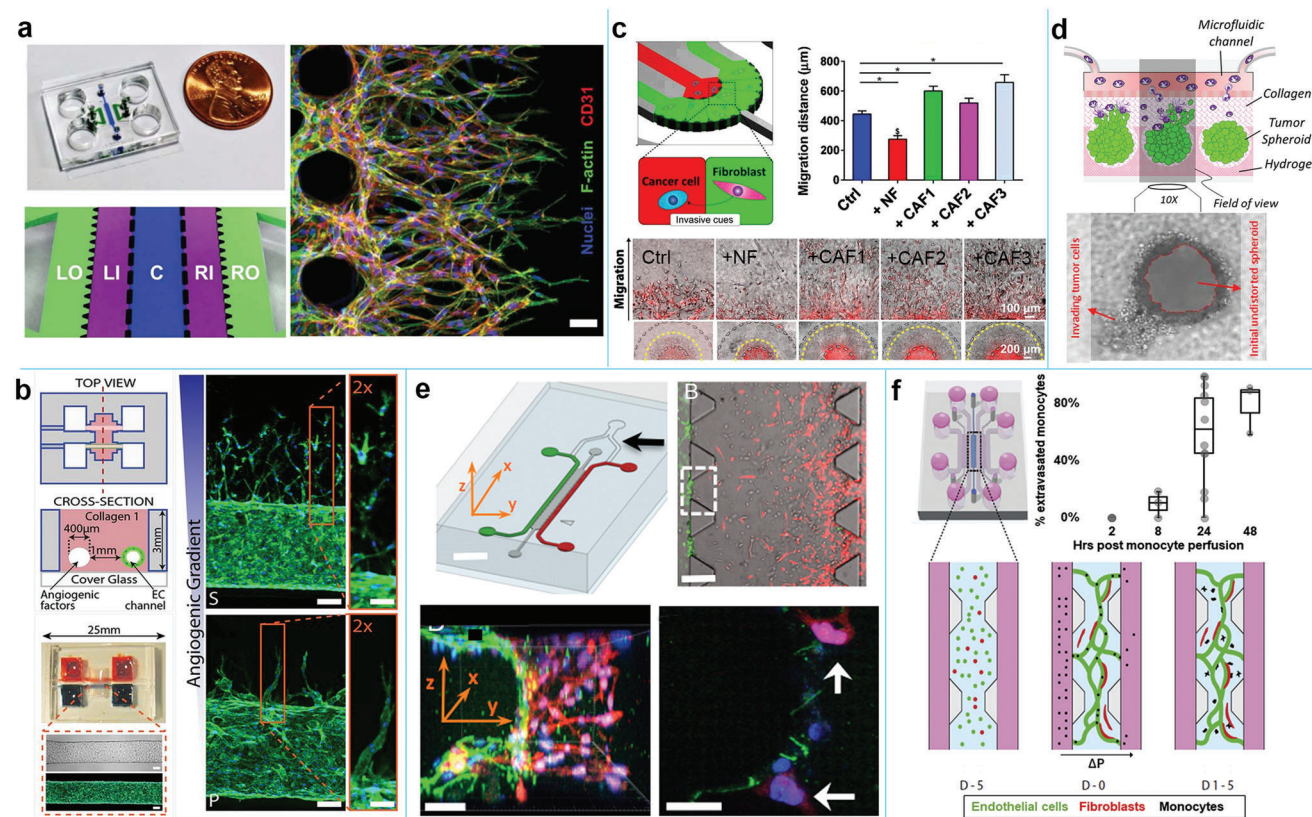


Figure 5. Microfluidic modeling of tumor metastasis. a) A microfluidic-based platform for capturing vasculogenic and angiogenic vessel formation. Scale bars: 100 μm . Reproduced with permission.^[112] Copyright 2013, Royal Society of Chemistry. b) Microfluidic lumen-based system for reconstituting angiogenesis in response to different proangiogenic factors. Scale bars: 100 μm . Reproduced with permission.^[114c] Copyright 2013, National Academy of Sciences. c) Organotypic microfluidic device for investigating tumor invasion in the presence of CAFs. Reproduced with permission.^[117] Copyright 2019, American Association for Cancer Research. d) Schematics of tumor-immune microenvironment in vitro: tumor spheroids are cocultured with neutrophils separated by porous membrane. Reproduced with permission.^[123] Copyright 2021, IOP Publishing. e) Hydrogel-based microfluidic platform modeling tumor intravasation. Reproduced with permission.^[127] Copyright 2012, National Academy of Sciences. f) A 3D vascularized microfluidic device replicating the effect of monocytes on tumor cell extravasation. Reproduced with permission.^[128] Copyright 2018, Elsevier.

gained increasing interest in multiplex screening of antiangiogenic drugs. Jeong et al. revealed that microRNA-497 exosome had the ability to significantly suppress the angiogenic sprouting of endothelial cells induced by a VEGF-A gradient in a microfluidic angiogenesis model.^[115] Similarly, the angiogenesis-on-a-chip was also employed for rapid and accurate assessment of RNA interference-based antiangiogenic nanomedicine.^[116] Overall, the microfluidic angiogenesis models can be utilized as valuable platforms for fundamental studies of tumor angiogenesis and for drug screening in kinetic analysis and clinical responses with physiological relevance.

Modeling Tumor Cell Invasion: To metastasize, cancer cells must degrade the surrounding ECM and then invade and migrate through the stroma. In this process, cancer cells will communicate with all components within the TME (e.g., endothelial cells, stromal cells, immune cells, hypoxia, chemokines, ECM composition, etc.) that regulate metastatic outcome. To date, microfluidic technology has been extensively used to reveal the roles of various cell types in tumor cell migration and invasiveness. In one study, a microfluidic device integrated with 3D hydrogel matrices was employed to determine the paracrine loop between hu-

man SUM159 breast carcinoma cells and patient-derived CAFs (Figure 5c).^[117] CAFs remarkably promoted breast tumor migration speed in a 3D matrix by inducing glycoprotein nonmetastatic B (GPNMB) expression in breast cancer cells. In another study, Lugo-Cintrón and co-workers incorporated normal breast fibroblasts and a fibronectin-rich matrix within a 3D microfluidic coculture system to investigate the combined influence of fibroblasts and different ECM compositions on breast cancer (MDA-MB-231) migration.^[118] The results illustrated that in the presence of normal breast fibroblasts, the number of migrating breast cancer cells within a fibronectin-rich matrix was significantly increased through the increased secretion of MMPs. In addition, noncancerous cells were also cocultured with corresponding cancer cells to study their role in cancer cell migration.^[119] It was shown that the presence of normal cells (MCF-10A or HDF-n) significantly increased the migration of MDA-MB-231 cells by increasing the expression level of IL-6 protein.

Apart from stromal cells, endothelial and immune cells also affected cancer cell invasion. An example was reported by Nagaraju et al., who developed a three-layer microfluidic device to coculture breast cancer cells (MDA-MB-231) and endothelial

cells (HUVECs) in different channels. Their findings demonstrated that the invasiveness of tumor cells was enhanced in the presence of spontaneously formed vasculature. Moreover, tumor cells' presence led to thinner and more permeable vessels forming, comparable to in vivo studies.^[120] In a more extensive study, Truong et al. leveraged the same microfluidic platform to investigate the crosstalk between glioma stem cells and endothelial cells.^[121] They observed that endothelial cells increased glioma stem cell invasion in 3D hydrogel via the CXCL12-CXCR4 signaling pathway. They compared this in vitro platform to in vivo mice model and found similar invasive behaviors, suggesting that their microfluidic platform presented a native-like microenvironment. Through coculturing macrophages with MDA-MB-231 cancer cells in a 3D microfluidic chip, Hebert et al. reported that macrophages could speed up cancer cell migration through secreting TGF- β 1.^[122] A similar finding was reported with the coculture of neutrophils with ovarian tumor cells in a microfluidic device (Figure 5d).^[123] Neutrophils promoted ovarian tumor cell invasion by generating neutrophil extracellular traps.

The biochemical and biophysical cues of TME also influence cancer cell invasion. Because of laminar flow and limited mass transport within 3D hydrogel, a microfluidic platform integrated with a 3D hydrogel matrix can establish stable chemical gradients for studying 3D chemotactic invasion. Sun et al. employed chemical reagents to generate an oxygen gradient for studying the effect of hypoxia on cancer cell migration in 3D culture. It was well recognized that hypoxia and fibroblasts jointly enhanced cancer cell migration.^[124] Using a novel microfluidic chip permitting side-by-side positioning of 3D hydrogel-based matrices, Truong et al. demonstrated that a transient gradient of epidermal growth factor significantly enhanced SUM159 breast cancer cell invasion.^[125] In a separate study, interstitial fluid pressure was found to promote collective tumor cell invasion in an engineered chip by increasing the expressions of Snail, E-cadherin, and Vimentin involved in EMT.^[126] These findings emphasize the importance of the chemical and physical cues in the dynamic modeling of in vivo TME for investigating tumor invasion.

Modeling Tumor Cell Intravasation and Extravasation: During metastasis, the steps involved in the transmigration of tumor cells across the endothelium have been defined as essential and possibly rate-limiting steps of the metastatic cascade. Therefore, various microfluidic tumor-vascular models have been developed to study cancer cell intravasation and extravasation. In one study, an intravasation model on a chip was developed to visualize the interaction between endothelial cells and invasive fibrosarcoma cells (HT1080) (Figure 5e). It was observed that carcinoma cell intravasation was significantly increased in the presence of macrophages due to the endothelial barrier impairment by macrophage-secreted TNF- α .^[127] Using a similar 3D vascularized microfluidic model, Boussommier-Calleja et al. investigated the impact of human monocytes on cancer cell extravasation (Figure 5f).^[128] Their results demonstrated that human monocytes directly decreased the extravasation of tumor cells in a noncontact-dependent manner. However, once monocytes transmigrated through the vasculature and became macrophage-like, they had little influence on tumor cell extravasation. This finding could be useful for exploring new antimetastatic therapeutic methods by targeting the crosstalk between monocytes and cancer cells.

The effect of other immune cells in facilitating tumor cell extravasation has also been presented in the microfluidic tumor-vascular models. In one study by Crippa et al., a human early metastatic niche-on-a-chip model was developed to study how neutrophils and platelets affected cancer cell extravasation. It was found that the presence of neutrophils and platelets dramatically enhanced the trans-endothelial migration of cancer cells.^[129] Recently, luminal and trans-endothelial fluid flows were also incorporated into a 3D microvascular platform to investigate their role in cancer cell extravasation. The authors found that luminal flow enhanced tumor cell extravasation via increased intravascular migration speed.^[130] In a different approach, a microfluidic lumen-based platform was developed to investigate the impact of cancer-vascular signaling cues on cancer extravasation.^[131] Their results demonstrated that the extravasation of breast cancer cells was promoted by the upregulation of several secreted factors such as IL-6, IL-8, and MMP-3.

Metastasis organ specificity and extravasation appear to be tightly coupled because specific chemo-attractant molecules are secreted by organ-specific stromal cells.^[132] To unveil the underlying mechanism of organ-specific metastasis, organ-specific human 3D microfluidic models have been established. For example, a three-channel microfluidic platform containing a microvascular network embedded in a bone-like or muscle-like microenvironment was used to study organ-specific cancer cell extravasation.^[132] The bone environment was created by coculturing primary human bone marrow-derived mesenchymal stem cells (BM-MSCs) and osteoblasts with endothelial cells in ECM. By contrast, the ECM gel of the muscle microenvironment was seeded with C2C12 myoblasts and HUVECs. It was found that the extravasation rate and vessel permeability were much higher in the bone-mimicking microenvironment than in the muscle-mimicking microenvironment. A deeper analysis revealed that the presence of C2C12-secreted adenosine significantly decreased the extravasation of cancer cells within the bone microenvironment. Similarly, Kwak and Lee modeled organotypic bone and lung metastasis in breast cancer on a microfluidic tumor-lumen device where subpopulations of MDA-MB-231 were introduced into a blood vessel surrounded by organ-specific parenchymal cells.^[133] Their results showed that the lung-mimicking microenvironment enhanced lung-tropic breast cancer extravasation, while the bone microenvironment with osteoblasts and BM-MSCs promoted the bone-tropic breast cancer extravasation. In addition, the Kamm group developed a brain-metastasis microvascular microfluidic model to understand the mechanisms of breast cancer extravasation through the BBB.^[134] They observed that astrocytes directly enhanced tumor cell extravasation across the BBB via C-C motif chemokine ligand 2 (CCL2) secretion, which was similar to in vivo observations. These findings indicate that this microfluidic metastatic platform has the potential to act as a robust, complementary approach to in vivo experiments.

Various microfluidic metastatic models have been developed to understand the cellular and molecular players in the complex metastasis cascade. However, the limitation is that most of them only captured one step of metastasis. More comprehensive microfluidic devices are needed to mimic in vivo metastasis process, especially multiorgan chips.

3.3.2. Microfluidic Modeling Response to Cancer Treatments

In the last decades, many microfluidic 3D tumor models have been developed to investigate how microenvironmental cues (e.g., stromal fibroblasts, vasculature, hypoxia) affect cancer cell responses to anticancer drugs. One 3D microfluidic invasion platform that compartmentalizes SUM159 breast cancer cells and stromal fibroblasts in a 3D gel was reported for assessing the efficacy of suberoylanilide hydroxamic acid (SAHA) in the treatment of solid tumors (Figure 6a).^[135] Using this model, the authors demonstrated that SAHA significantly reduced the migration of SUM159 breast cancer cells even in the presence of CAFs, suggesting that CAFs had no effect on drug resistance. Another microfluidic model integrating cancer cells with fibroblasts in proximity within a hydrogel matrix revealed that compared to monoculture, cancer cells cocultured with fibroblasts had a higher level of fibronectin expression with reduced drug uptake.^[136]

Apart from stromal fibroblasts, vasculature in the TME is also crucial for drug delivery and cancer cell survival because anticancer therapeutics need transport across the endothelial barrier to tumor sites. Furthermore, microvascular dysfunction resulting from anticancer drug treatment in turn reduces treatment efficacy. Therefore, the development of 3D vascularized tumor models on a chip for testing drug response has been attracting more attention in recent years. For example, Agarwal et al. engineered a 3D vascularized tumor model by integrating modular avascular microtumors and stromal cells (endothelial cells and human adipose mesenchymal/stromal stem cells) into a microfluidic device.^[72] This platform was utilized for testing the anticancer efficacy of free doxorubicin and doxorubicin-encapsulated NPs. It was demonstrated that the vascularized 3D tumors were more resistant to free doxorubicin than 2D-cultured cancer cells and avascular microtumors, while this effect was significantly diminished by nanoparticle-mediated drug delivery (Figure 3d). These results proved the importance of replicating the TME in evaluating treatment efficacy. Another similar study by Nashimoto et al.^[81] also revealed that the perfusable vascular network significantly enhanced tumor cell survival at a low dose of paclitaxel compared to that without vasculature, further demonstrating the importance of the stroma in drug delivery. In addition, a microfluidic device coupling 3D tumor spheroids with an oxygen gradient was developed to study how oxygen levels influence the cytotoxicity of two chemotherapeutic drugs (doxorubicin (Dox) and tirapazamine (TPZ)) in breast tumor spheroids (Figure 6b).^[68a] It was found that tumor cell survival in Dox treatment remarkably increased under low oxygen conditions, while TPZ showed higher cytotoxicity under hypoxia, which was consistent with *in vivo* data. These findings indicated that this platform might provide a better prediction of drug cytotoxicity under different oxygen levels.

Organoid-on-a-chip platforms have also been developed to evaluate the efficacy of anticancer therapeutics.^[103,137] An automated high-throughput microfluidic device was developed for drug screening on patient-derived pancreatic tumor organoids.^[105] Using this system, the authors observed that significant differences in the response of individual PDOs to specific drug treatments and dynamic drug treatments could be more effective than constant-dose therapy *in vitro*, indicating that this platform holds great potential to make clinical decisions for per-

sonalized therapy. Similarly, another microfluidic chip integrating organoid-culturing arrays and a concentration gradient generator was developed by Prince et al. for multiplexed anticancer drug testing (Figure 6c).^[106] Using this device, massive arrays of breast cancer organoids from two patients could be efficiently generated in a biomimetic hydrogel (within 72 h) and the drug sensitivity of patient-derived organoids in this platform captured *in vitro* and *in vivo* drug efficacy. These results demonstrated that this microfluidic platform could be utilized for antitumor drug screening and the development of personalized cancer therapies.

The variability of patient response to specific drugs poses a challenge in cancer treatments due to inter-patient tumor heterogeneity. To overcome this problem, patient-specific organotypic models *in vitro* also emerge for drug screening. For example, Jiménez-Torres et al. reported an organotypic blood vessel model from patient-derived normal endothelial cells and tumor endothelial cells for testing antiangiogenic drugs in RCC (Figure 6d).^[138] In this work, vessels were treated with two popular antiangiogenic agents (e.g., pazopanib and sunitinib) for RCC. They found that vessels from individual patients showed a highly variable response and dose dependence to these two drugs, highlighting the importance of creating a more personalized model for predicting drug efficacy. In another study from the same group, the authors further demonstrated the ability of their model to replicate phenotypic differences between normal and tumor-associated blood vessels.^[139] They identified two alternative therapeutics (nintedanib and sirolimus) with the potential to target tumor-associated vessels.

In another example, combination therapies were evaluated by engineering a microfluidic organotypic model that incorporated tumor spheroids isolated from patient-derived xenograft (PDX) models of HER2-mutant nonsmall cell lung cancer in a 3D collagen environment.^[140] This system could rapidly identify the efficacy of neratinib-based drug combinations (e.g., neratinib/trastuzumab and neratinib/temsirolimus), and the findings correlated well with HER2-mutated PDX models, suggesting that this *in vitro* system potentially predicts *in vivo* drug efficacy.

Although these models provide a powerful platform for screening anticancer therapeutics and facilitating individual treatment decisions, other microenvironmental factors of TME, such as CAFs, are not incorporated into these models. Most recently, Beebe group developed a microfluidic organotypic coculture model with lymphatic endothelial cells and CAFs isolated from head and neck cancer patients.^[141] Using this device, they found that IGF-1, a lymphangiogenic gene, was upregulated among all patients, while the anti-IGF-1 treatment was ineffective at reducing lymphangiogenesis or permeability across different patients, suggesting that personalized treatment for individual patients is required.

Despite the massive advancements in chemotherapies in the last decades, the efficacy is far from satisfactory due to poor accumulation in tumor sites, nonspecific toxicity, and drug resistance.^[142] To address these therapeutic issues, nanoparticles (NPs) for chemotherapeutic agent delivery are applied to cancer treatments due to their remarkable advantages in increasing drug solubility, improving the bioavailability of drugs, reducing nonspecific toxicity, and prolonging circulation time.^[143] Various 3D microfluidic chip-based *in vitro* models have also been reported

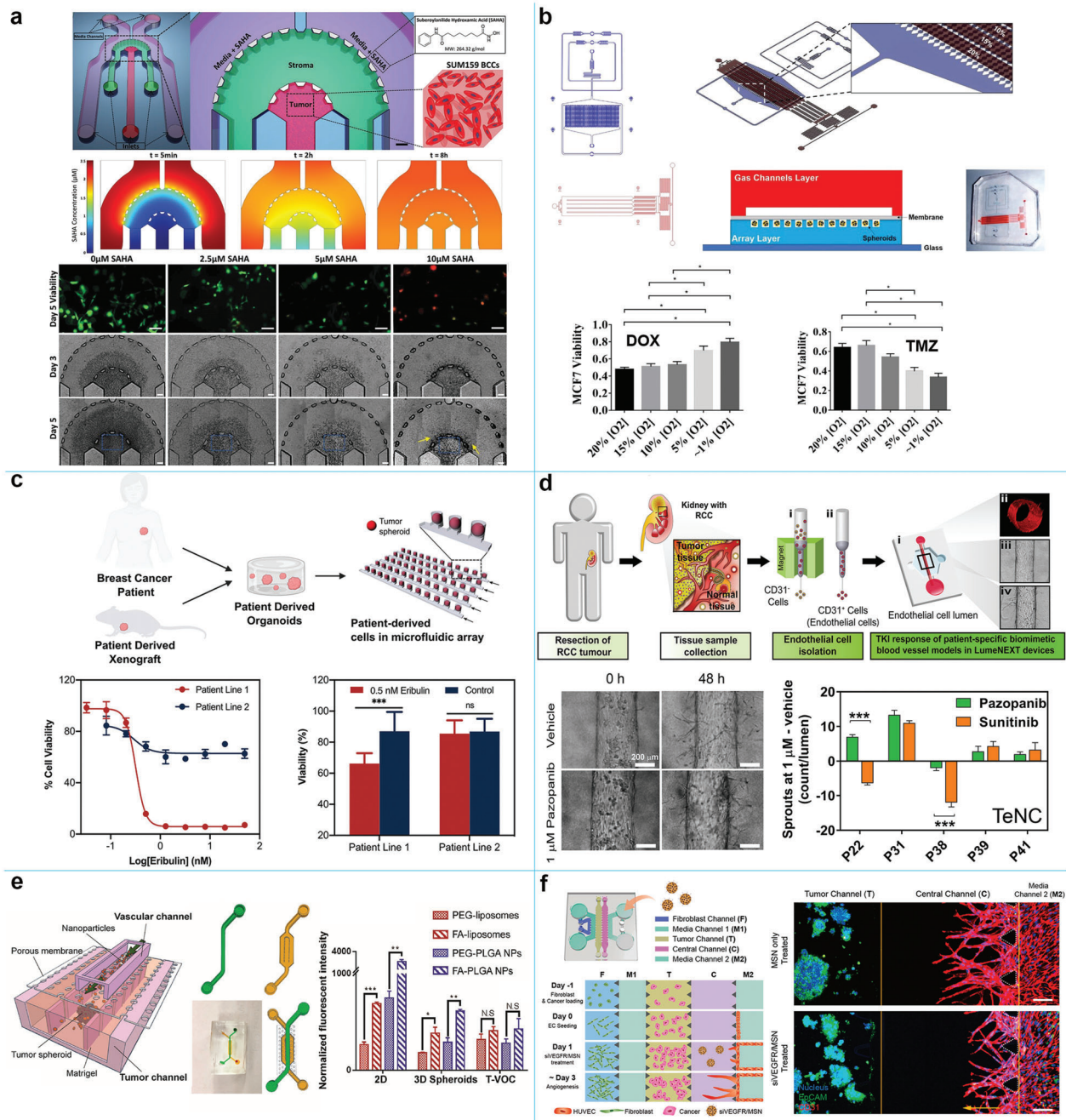


Figure 6. Microfluidic modeling of tumor response to therapeutics. a) Microfluidic invasion model that captures the crosstalk between tumor cells and CAFs for anticancer drug studies. Scale bar is 125 μm . Reproduced with permission.^[135] Copyright 2017, Royal Society of Chemistry. b) Schematics of oxygen gradient-array microfluidic device for studying the effect of oxygen levels on drug cytotoxicity in tumor spheroids. Reproduced with permission.^[68a] Copyright 2021, IOP Publishing. c) Illustration of microfluidic arrays to generate PDOs for developing personalized cancer therapies. Reproduced with permission.^[106] Copyright 2021, Wiley-VCH GmbH. d) Microfluidic lumen-based system for evaluating anti-angiogenesis treatment in RCC patients. Reproduced with permission.^[138] Copyright 2019, Elsevier. e) Tumor-vasculature-on-a-chip for drug-loaded nanoparticles evaluation. Reproduced with permission.^[144] Copyright 2018, American Chemical Society. f) 3D microfluidic cancer angiogenesis-on-a-chip for RNAi-based nanomedicine evaluation. Scale bar is 200 μm . Reproduced with permission.^[116] Copyright 2021, American Chemical Society.

to assess the efficacy and safety of anticancer drug-loaded nanoparticles in a more physiological environment. For example, a tumor-vasculature-on-a-chip model containing ovarian tumor spheroids embedded in the bottom gel channel and endothelial cells seeded in the top channel was developed to study NP extrava-

sation and tumor accumulation (Figure 6e).^[144] This setup captured the key biological barriers involved in NP delivery in vivo, including the leaky tumor vasculature and dense extracellular matrix. Using this device, the authors found that the presence of these two barriers significantly decreased the permeability of NPs

compared to the individual barrier of leaky vasculature and dense tumor ECM. Furthermore, the cellular uptake of targeted and untargeted NPs in tumor spheroids exhibited no significant differences in this model, which was in line with findings in animal models. In another study, a microfluidic tumor vascular model was engineered by Jeon group for the accurate evaluation of RNA interference-based antiangiogenic nanomedicine (Figure 6f).^[116] It was demonstrated that the siVEGFR-loaded nanoparticles effectively inhibited the angiogenic sprouting without affecting the viability of endothelial cells.

Taken together, all these results suggested that 3D microfluidic tumor models can serve as a reliable and predictive platform for assessing anticancer therapeutics (e.g., molecular, NP-based, and cellular therapies.), investigating combinatorial drug therapy, and developing personalized treatments in an in vivo-like TME. Moreover, given the excellent control of fluid flow, the vascularized tumor chips are particularly helpful in studying how tumors respond to drugs in a physiological blood flow condition.

3.3.3. Microfluidic Modeling Blood–Brain Barrier

Glioblastoma (GBM) remains the most aggressive primary brain cancer, with a median survival of 12–15 months.^[145] The standard of care for GBM is surgical resection followed by radiation therapy and chemotherapy, but only limited success has been achieved. One major reason is the presence of the highly selective, semipermeable blood–brain barrier in the central nervous system (CNS). The BBB is a physiological barrier between peripheral blood circulation and the CNS to protect the brain from pathogens and toxins, enabling retain the brain homeostasis. Compared to the typical blood vessels in other human organs, the BBB is more complex and composed of endothelial cells (ECs), pericytes (PCs), supporting glial cells (astrocytes (ACs) and microglia), basement membranes, and the ECM, which are indispensable for retaining the BBB integrity. The BBB restricts the delivery of most substances to the brain and thereby limits the therapeutic efficacy of most chemotherapies. To explore efficient therapeutic strategies that can penetrate the BBB, a deeper understanding of this multicellular and complex barrier is needed. Current BBB studies prominently depend on in vitro cell-based models and in vivo animal models. However, these approaches suffer from low throughput, ethics concerns, or lack of physiological relevance, respectively. Thereby, developing a 3D in vitro BBB model that could faithfully emulate the structure and function of the BBB is urgent.

Design of 3D BBB Microfluidic Models: In terms of structural design, current 3D BBB-on-a-chip platforms can be divided into four types:^[145] 1) sandwiched design with an upper vascular and a lower brain layer separated by a porous membrane; 2) parallel design with aligned channels connected by PDMS microchannels or micropillars; 3) tubular design with circular cross-section lumens in a 3D matrix, and 4) vasculogenesis designs with neovascular network formation within gels. Although sandwiched and parallel designs are the two most commonly used models to recreate the human brain physiology, most of the microchannels are rectangular, resulting in nonuniform shear stress profiles along the vascular endothelium. An improved strategy is developing gel-based 3D BBB devices with cylindrical microchan-

nels by using microneedles as templates or viscous finger patterning. Such tubular vascular structure enables constant flow along the lumen. In addition, the vasculogenesis strategy has also been explored to reconstruct 3D neurovascular networks. In this approach, endothelial cells self-organize into in vivo-like capillary networks in gel-filled channels.

As mentioned above, all cell types involved in the neurovascular unit are indispensable for maintaining the BBB integrity. Therefore, to design an appropriate BBB model, the selection of cell types and sources should be taken into consideration. Initially, ECs and ACs isolated from rat, bovine, and porcine were utilized to construct functional BBB.^[146] In one study, Adriani and coworkers engineered a 3D neurovascular microfluidic model by incorporating a compartmentalized 3D monolayer of human ECs in coculture with primary rat ACs and neurons (Figure 7a).^[147] As a result, a structural in vitro BBB model with size-selective permeability was generated, but this platform lacked in vivo-like direct interfaces between vascular networks and astrocytes. As such, a novel 3D BBB-on-a-chip model with direct contact between astrocytes and a perusable vascular network was proposed by embedding HUVECs in a fibrin hydrogel and coculturing rat neural cells (ACs and neurons) in an adjacent channel (Figure 7b).^[148] It was observed that direct interaction with rat neural cells was responsible for low permeability. However, these models have some drawbacks. First, HUVECs form a leakier barrier than brain endothelial cells.^[147,149] Second, using rat neural cells in these models may pose cross-species compatibility. Third, PCs are not considered in these models while they are recognized as a critical component of the BBB.^[150]

To address these limitations, Jeon group proposed a microfluidic in vitro BBB system with primary human cells (brain ECs, hPCs, and hACs) through angiogenesis (Figure 7c).^[151] It was confirmed that tri-culture of brain ECs with pericytes and astrocytes was essential for maintaining BBB phenotypes such as narrow vascular morphology, low vascular permeability, and functional efflux transporter. Human primary cells are ideal but expensive and difficult to obtain. Alternatively, human-induced pluripotent stem cell-derived endothelial cells (iPSC-ECs) with self-renewal capability hold great potential in constructing BBB models in vitro. A 3D BBB microvascular network model was engineered with the coculture of human iPSC-ECs, brain ACs, and PCs in a 3D fibrin hydrogel (Figure 7d),^[152] which showed that a perfusable and well-connected microvascular network (μ VN) was formed via the self-organization of all cell types. Moreover, direct interaction of the μ VN with human neural cells has rendered the microvasculature with low permeability, comparable to that present in rat brains. Taken together, the authors provided a robust and reliable method to establish more physiologically relevant BBB models.

Applications in Modeling Brain Tumors And Metastasis: Initially, most studies rely only upon coculturing of glioma stem cells (GSCs) with ECs to mimic the glioma microenvironment. As a way to study GSCs-vascular crosstalk, Truong et al. designed a 3D organotypic microfluidic model by coculturing patient-derived GSCs and HUVECs in hydrogel-filled chambers.^[153] They demonstrated that the well-established microvascular network boosted GSC invasion as well as maintained GSC proliferation ability and stemness phenotype. Importantly, GSC invasion in this microfluidic platform was consistent with those

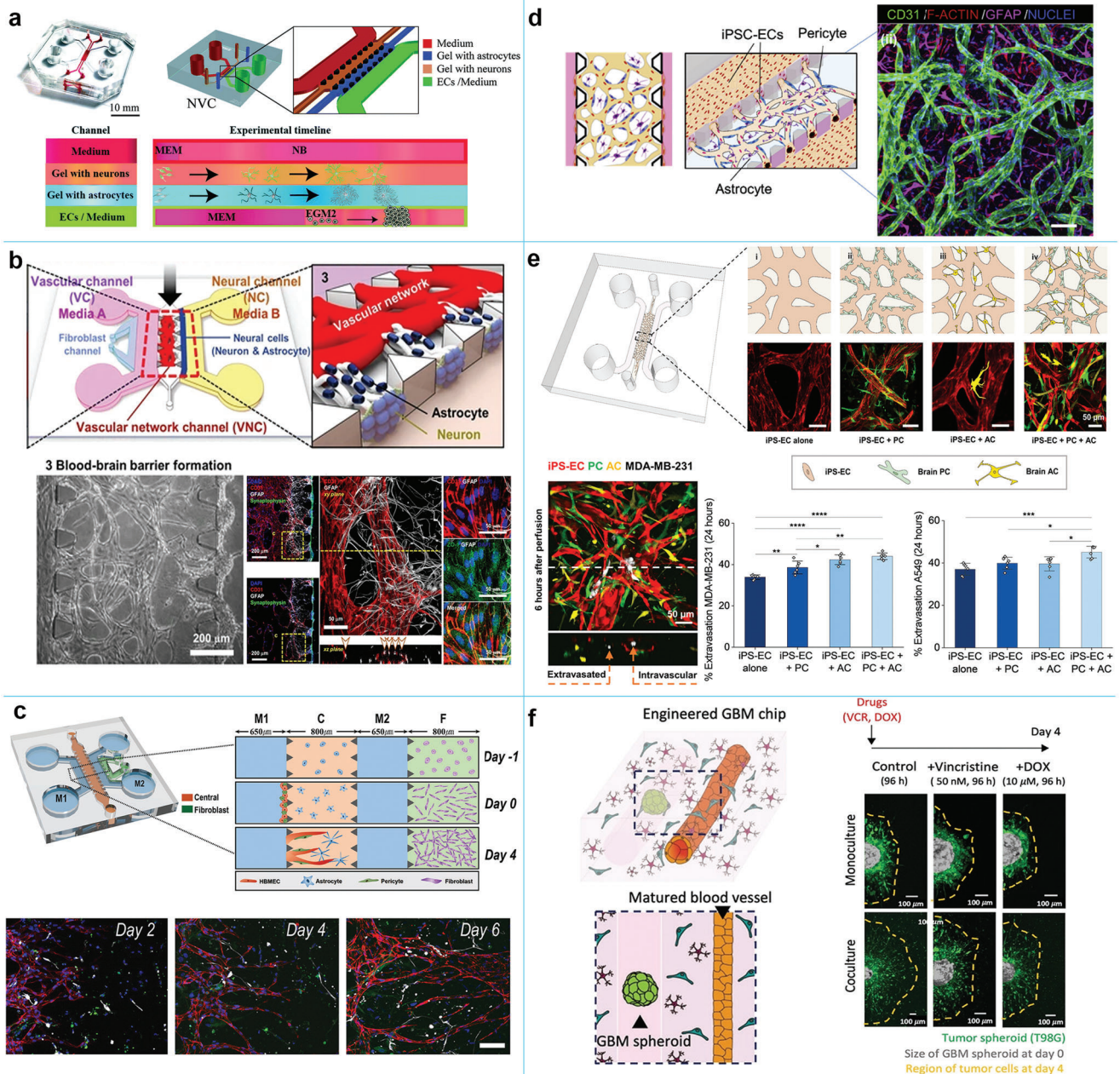


Figure 7. Microfluidic modeling of blood–brain barrier. a) A 3D neurovascular microfluidic model consisting of HUVECs, rat neurons and astrocytes. Reproduced with permission.^[147] Copyright 2017, Royal Society of Chemistry. b) A low permeability microfluidic BBB platform incorporating vascular networks and rat neural cells (neurons and astrocytes). Reproduced with permission.^[148] Copyright 2017, Springer Nature. c) Schematic representation of a microfluidic brain angiogenesis model containing human brain endothelial cells and human neural cells. Scale bar = 100 μm. Reproduced with permission.^[151] Copyright 2019, Wiley. d) Schematic view of 3D BBB microvascular network model mimicking the microvascular structure present in the brain environment. Scale bars: 100 μm. Reproduced with permission.^[152] Copyright 2018, Elsevier. e) Schematics of a 3D in vitro BBB microvascular model to study brain metastasis. Reproduced with permission.^[134] Copyright 2021, American Association for the Advancement of Science. f) Microfluidic lumen-based BBB model to evaluate drug response of GBM spheroids. Reproduced with permission.^[159] Copyright 2021, Wiley-VCH GmbH.

observed *in vivo*, suggesting this system could represent a physiologically relevant *in vitro* microenvironment. Lin et al. sought to design a GBM-on-a-chip for mimicking the glioma immune niche through incorporating glioma cells, endothelial cells, and macrophages in hydrogel-based biomaterials.^[154] Using the device, the authors were able to separately observe the morphol-

ogy change and migration of glioma cells in the presence of macrophages. It is worth noting that the majority of these studies did not include other supporting niche-specific cell types, such as ACs, and PCs. To create a realistic and complex microenvironment model, Adjei-Sowah et al. proposed an organotypic tri-culture microfluidic model containing ECs, ACs, and GSCs.^[155]

Using single-cell RNA sequencing, 15 ligand–receptor pairs were identified to be related to the chemotactic invasion of GSCs toward the perivascular niche.

The BBB models have also been utilized to advance our insight into the mechanisms involving brain metastases of malignant cancer cells. For example, by using a sandwiched design, Altemus et al. observed the whole process of breast tumor metastasis to the brain and found that the integrity of BBB could be compromised by invading cancer cells.^[156] However, the use of sandwiched design comes with some drawbacks—its difficulty to achieve high-resolution images due to the cell seeding configuration and low-throughput screening. To overcome these drawbacks, Xu et al. designed a BBB-on-a-chip using the parallel design.^[146] In this study, several cancer cell types were introduced into the vascular compartment to mimic the procedure of tumor cell extravasation across the BBB. It was demonstrated that lung cancer, breast cancer, and melanoma cells could cross the BBB while liver cancer did not.^[146] Further advancement in microfluidic modeling brain metastases is by designing a 3D in vitro BBB microvascular model through coculture of all relevant cell types in the BBB to explore cancer extravasation at the brain (Figure 7e).^[134] Using this triculture BBB model, the researchers found that the presence of astrocytes in the microvascular networks directly promoted tumor cell transmigration into the brain tissue through their secretion of CCL2.

Applications in Evaluating GBM Therapies: Owing to restricted transport of therapeutics across the BBB, developing new drugs for effectively targeting brain tumors is a current research hotspot. Kamm group designed and fabricated a microfluidic 3D in vitro human BBB model composed of self-assembled human ECs, ACs, and PCs to quantify nanoparticle delivery across the human BBB.^[157] It was found that this platform allowed for a more rapid assessment of PEG-coated nanoparticle transport to the brain than using a 2D transwell setup (5 min vs 3 h). Furthermore, surface modification of NPs with holo-transferrin enhanced NP accumulation in brain tissue, suggesting its potential to screen preclinical nanotherapeutics. To precisely predict the performance of drugs in human patients, the same group recently engineered an in vitro vascularized GBM-on-a-chip featuring GBM spheroids embedded in a self-assembled BBB vasculature.^[158] Using this model, the authors observed close-to-physiology brain tumor vasculature with low permeability and enhanced junction and transport protein expression. More importantly, this model allowed assessing the GBM-targeting ability of surface-functionalized nanomedicines in a realistic setting. It was demonstrated that these functionalized nanoparticles improved efficacy and targeted delivery of encapsulated cisplatin both in vitro and in vivo. Another different GBM model was designed by incorporating brain tumor spheroids into a lumen-based BBB chip (Figure 7f).^[159] Using this model, the authors studied the effect of the human GBM environment on tumor behaviors and drug response. They found that the brain tumor spheroids (T98G) cocultured with BBB-composing cells displayed more aggressiveness, higher drug resistance, and produced higher concentrations of inflammatory cytokines. Moreover, the transport of BBB-nonpenetrating drugs could be enhanced via chemically opened BBB. All these results indicated that advanced 3D GBM models might be used as robust in vitro platforms to investigate the mechanism of GBM

and monitor drug responses under the crosstalk of the BBB with brain tumor. In addition, the efficacy of programmed cell death protein-1 (PD-1) checkpoint immunotherapy was also evaluated on a patient-derived GBM-on-a-chip model, which consisted of two peripheral regions for vascular growth and middle regions for GBM growth.^[160] Using this platform, the researchers dissected macrophage-mediated angiogenesis and immunosuppression involved in regulating resistance to immunotherapy.

4. Challenges and Future Perspectives

Over the past decade, tremendous efforts have been focused on developing and validating various biomimetic in vitro 3D tumor models ranging from homotypic spheroids to heterogeneous organoids and complex perfusable tumor-on-a-chip. The advancement in biofabrication technologies allows these 3D tumor models to exhibit physiologically similar features to in vivo tumors in terms of tissue-specific ECM and biomimetic tumor microstructure. Although these models have deepened our insight into cancer biology and accelerated anticancer drug development, some limitations still need to be addressed before they find widespread applications.

First, tumor vasculature should be incorporated to predict drug efficacy as it plays an instrumental role in tumor growth and metastasis. Fortunately, with the development of biofabrication techniques, microfluidic and 3D bioprinting technologies have been employed to create more in vivo-like perfusable 3D tumor models in the biomimetic matrix.^[72,161] Nonetheless, these approaches are still in the initial stages and should be further explored in the field of vascularized cancer modeling. Meanwhile, other key aspects, including reproducibility, long-term culture, and scalability into high-throughput screening, should also be considered for establishing spheroids/organoids with functional and perfusable vascular systems.

Second, the native TME with tissue-specific ECM composition and dynamically tunable mechanical properties should be taken into consideration. To date, various natural and synthetic hydrogels have been adopted for engineered tumor tissues, including Matrigel, collagen, fibrin, alginate, PEG, etc. However, these compositions are inherently distinct from that of the native TME. A creative solution to this challenge is using decellularized matrix isolated from patient tumor tissues.^[99b,162] Notably, the mechanical stiffness of the surrounding ECM is constantly increasing during tumor progression. Increasing matrix stiffness has been demonstrated to be correlated with tumor proliferation and chemotherapeutic resistance.^[163] More recently, another interesting mechanical property, stress relaxation, was also shown to affect cell fate and drug response.^[164] As such, the supporting matrix for 3D culture should mimic both biochemical and biophysical cues of the native TME.

Third, in vitro models that are based on patient-derived cancer cells are urgently needed. The high inter- and inpatient heterogeneity leads to a large variability in patients' responses to cancer treatments. This calls for a need to model the TME using patient-derived cells or iPSC-derived cells. However, developing such models is still challenging because different cell types require specific isolation protocols and culture conditions to maintain their functions. A recent study for breast cancer demonstrated that this could be improved through

medium optimization.^[84] However, it is still uncertain whether this method may be expanded to other cancer types and how the efficiency of organoid formation is. In addition, CTC-derived tumors also attracted increasing attention as they share histological and immunohistochemical features of the donor patient tumor,^[165] but their culture conditions remain to be optimized.

Fourth, the standardization of the models raises another important point. To adequately reflect the human TME, the models are required to contain the most necessary components and biochemical/biophysical factors, which would generally sacrifice fidelity and throughput and pose another challenge for drug discovery and testing. As such, it is necessary to find a balance between automation and complexity for diverse applications. Additionally, current cancer on-a-chip platforms rely much on PDMS, while it suffers from nonspecific absorption of drugs and proteins, driving its use away from drug screening. Further innovation on novel materials and robust rapid prototyping techniques continues to be required. In addition to scalability, the integration of functional biosensors or standard equipment with these systems is necessary, which will speed up the automation and boost their potential for clinical translation.

Finally, another critical concern in engineering more robust tumor chips is by creating multiorgan-on-a-chip. By using this type of model, the side effects of anticancer drugs can be examined.^[166] This system has also provided a promising tool for studying the crosstalk between tumor metastasis and distant organs,^[167] but the development of a universal culture medium that sustains cell viability and functionality across different types of organ chips for a long time remains a considerable challenge.

5. Conclusions

In this review, we have summarized recent advances in the establishment of 3D in vitro cancer models. Various cancer models have been engineered to mimic the complexity of TME, including ECM composition, hypoxia, interstitial flow, and cell–cell interactions. Although there are still many barriers on the road to engineering pathologically relevant in vitro models, the models reported so far have already advanced fundamental cancer research and paved the way for preclinical studies and drug discovery. With the development of next-generation biomaterials and microfabrication technologies, we envision that more physiologically representative 3D tumor models could be created in the future by coupling multiple technologies, including microfluidics, 3D bioprinting, hydrogel engineering, and spheroid/organoid techniques.

Acknowledgements

This work was supported by grants from Hetao Shenzhen-Hong Kong Science and Technology Innovation Cooperation Zone Shenzhen Park Project (HZQB-KCZY2021017), the Research Impact Fund of the Hong Kong Research Grant Council (R1020-18F), and City University of Hong Kong (Project #9678223).

Conflict of Interest

The authors declare no conflict of interest.

Keywords

in vitro models, organoids, spheroids, tumor microenvironment, tumor-on-a-chip

Received: October 11, 2022

Revised: February 22, 2023

Published online: March 29, 2023

- [1] H. Sung, J. Ferlay, R. L. Siegel, M. Laversanne, I. Soerjomataram, A. Jemal, F. Bray, *CA Cancer J. Clin.* **2021**, *71*, 209.
- [2] a) C. H. Wong, K. W. Siah, A. W. Lo, *Biostatistics* **2019**, *20*, 273; b) C. Toniatti, P. Jones, H. Graham, B. Pagliara, G. Draetta, *Cancer Discovery* **2014**, *4*, 397.
- [3] M. Simian, M. J. Bissell, *J. Cell Biol.* **2017**, *216*, 31.
- [4] A. Riedl, M. Schleder, K. Pudilko, M. Stadler, S. Walter, D. Unterleuthner, C. Unger, N. Kramer, M. Hengstschläger, L. Kenner, *J. Cell Sci.* **2017**, *130*, 203.
- [5] a) K. Chitcholtan, E. Asselin, S. Parent, P. H. Sykes, J. J. Evans, *Exp. Cell Res.* **2013**, *319*, 75; b) T. W. Ridky, J. M. Chow, D. J. Wong, P. A. Khavari, *Nat. Med.* **2010**, *16*, 1450.
- [6] a) Y. Yoshii, T. Furukawa, A. Waki, H. Okuyama, M. Inoue, M. Itoh, M.-R. Zhang, H. Wakizaka, C. Sogawa, Y. Kiyono, *Biomaterials* **2015**, *51*, 278; b) S. Melissaridou, E. Wiechec, M. Magan, M. V. Jain, M. K. Chung, L. Farnebo, K. Roberg, *Cancer Cell Int.* **2019**, *19*, 16.
- [7] L. Kelland, *Eur. J. Cancer* **2004**, *40*, 827.
- [8] Y. Zhao, T. W. H. Shuen, T. B. Toh, X. Y. Chan, M. Liu, S. Y. Tan, Y. Fan, H. Yang, S. G. Lye, G. K. Bonney, *Gut* **2018**, *67*, 1845.
- [9] I. W. Mak, N. Evaniew, M. Ghert, *Am. J. Transl. Res.* **2014**, *6*, 114.
- [10] S. Wang, D. Gao, Y. Chen, *Nat. Rev. Urol.* **2017**, *14*, 401.
- [11] A. Sontheimer-Phelps, B. A. Hassell, D. E. Ingber, *Nat. Rev. Cancer* **2019**, *19*, 65.
- [12] S. M. Kang, D. Kim, J. H. Lee, S. Takayama, J. Y. Park, *Adv. Healthcare Mater.* **2021**, *10*, 2001284.
- [13] V. Veninga, E. E. Voest, *Cancer Cell* **2021**, *39*, 1190.
- [14] L. Wan, C. A. Neumann, P. R. LeDuc, *Lab Chip* **2020**, *20*, 873.
- [15] R. K. Jain, *Science* **2005**, *307*, 58.
- [16] M. Wang, Y. Liu, Y. Cheng, Y. Wei, X. Wei, *Biochim. Biophys. Acta.* **2019**, *1871*, 199.
- [17] D. O. Bates, T.-G. Cui, J. M. Doughty, M. Winkler, M. Sugiono, J. D. Shields, D. Peat, D. Gillatt, S. J. Harper, *Cancer Res.* **2002**, *62*, 4123.
- [18] S. J. Turley, V. Cremasco, J. L. Astarita, *Nat. Rev. Immunol.* **2015**, *15*, 669.
- [19] K. Räsänen, A. Vaheri, *Exp. Cell Res.* **2010**, *316*, 2713.
- [20] E. L. Spaeth, J. L. Dembinski, A. K. Sasser, K. Watson, A. Klopp, B. Hall, M. Andreeff, F. Marini, *PLoS One* **2009**, *4*, e4992.
- [21] R. Kalluri, M. Zeisberg, *Nat. Rev. Cancer* **2006**, *6*, 392.
- [22] E. M. Zeisberg, S. Potenta, L. Xie, M. Zeisberg, R. Kalluri, *Cancer Res.* **2007**, *67*, 10123.
- [23] J. Vaquero, N. Guedj, A. Clapéron, T. H. N. Ho-Bouldoires, V. Paradis, L. Fouassier, *J. Hepatol.* **2017**, *66*, 424.
- [24] A. Orimo, P. B. Gupta, D. C. Sgroi, F. Arenzana-Seisdedos, T. Delaunay, R. Naeem, V. J. Carey, A. L. Richardson, R. A. Weinberg, *Cell* **2005**, *121*, 335.
- [25] a) A. D. Rhim, P. E. Oberstein, D. H. Thomas, E. T. Mirek, C. F. Palermo, S. A. Sastra, E. N. Dekleva, T. Saunders, C. P. Becerra, I. W. Tattersall, *Cancer Cell* **2014**, *25*, 735; b) Y. Mizutani, H. Kobayashi, T. Iida, N. Asai, A. Masamune, A. Hara, N. Esaki, K. Ushida, S. Mii, Y. Shiraki, *Cancer Res.* **2019**, *79*, 5367.
- [26] a) E. M. Dijkgraaf, M. Heusinkveld, B. Tummers, L. T. Vogelpoel, R. Goedemans, V. Jha, J. W. Nortier, M. J. Welters, J. R. Kroep, S. H. van der Burg, *Cancer Res.* **2013**, *73*, 2480; b) T. Shree, O. C. Olson,

- B. T. Elie, J. C. Kester, A. L. Garfall, K. Simpson, K. M. Bell-McGuinn, E. C. Zabor, E. Brogi, J. A. Joyce, *Genes Dev.* **2011**, *25*, 2465; c) D. G. DeNardo, D. J. Brennan, E. Rexhepaj, B. Ruffell, S. L. Shiao, S. F. Madden, W. M. Gallagher, N. Wadhvani, S. D. Keil, S. A. Junaid, *Cancer Discovery* **2011**, *1*, 54.
- [27] D. M. Mosser, J. P. Edwards, *Nat. Rev. Immunol.* **2008**, *8*, 958.
- [28] a) C. Subimerb, S. Pinlaor, N. Khuntikeo, C. Leelayuwat, A. Morris, M. S. McGrath, S. Wongkham, *Mol. Med. Rep.* **2010**, *3*, 597; b) K. Yamamoto, T. Makino, E. Sato, T. Noma, S. Urakawa, T. Takeoka, K. Yamashita, T. Saito, K. Tanaka, T. Takahashi, *Cancer Sci.* **2020**, *111*, 1103.
- [29] N. R. Anderson, N. G. Minutolo, S. Gill, M. Klichinsky, *Cancer Res.* **2021**, *81*, 1201.
- [30] E. Mavrogatou, H. Pratsinis, A. Papadopoulou, N. K. Karamanos, D. Kletsas, *Matrix Biol.* **2019**, *75*, 27.
- [31] a) E. Henke, R. Nandigama, S. Ergün, *Front. Mol. Biosci.* **2020**, *6*, 160; b) S. Nallanthighal, J. P. Heiserman, D.-J. Cheon, *Front. Cell. Dev. Biol.* **2019**, *7*, 86.
- [32] G. Bahcecioglu, G. Basara, B. W. Ellis, X. Ren, P. Zorlutuna, *Acta Biomater.* **2020**, *106*, 1.
- [33] V. Poltavets, M. Kochetkova, S. M. Pitson, M. S. Samuel, *Front. Oncol.* **2018**, *8*, 431.
- [34] R. Grantab, S. Sivanathan, I. F. Tannock, *Cancer Res.* **2006**, *66*, 1033.
- [35] M.-Z. Jin, W.-L. Jin, *Signal Transduction Targeted Ther.* **2020**, *5*, 166.
- [36] J. M. Brown, W. R. Wilson, *Nat. Rev. Cancer* **2004**, *4*, 437.
- [37] a) H. Kim, Q. Lin, P. M. Glazer, Z. Yun, *Breast Cancer Res.* **2018**, *20*, 16; b) C. Zhang, D. Samanta, H. Lu, J. W. Bullen, H. Zhang, I. Chen, X. He, G. L. Semenza, *Proc. Natl. Acad. Sci. USA* **2016**, *113*, E2047.
- [38] a) G. L. Semenza, *Nat. Rev. Cancer* **2003**, *3*, 721; b) A. Giaccia, B. G. Siim, R. S. Johnson, *Nat. Rev. Drug Discovery* **2003**, *2*, 803.
- [39] M. L. Shang, R. H. Soon, C. T. Lim, B. L. Khoo, J. Han, *Lab Chip* **2019**, *19*, 369.
- [40] C.-H. Heldin, K. Rubin, K. Pietras, A. Östman, *Nat. Rev. Cancer* **2004**, *4*, 806.
- [41] M. Milosevic, A. Fyles, D. Hedley, M. Pintilie, W. Levin, L. Manchul, R. Hill, *Cancer Res.* **2001**, *61*, 6400.
- [42] a) S. Kim, M. Chung, J. Ahn, S. Lee, N. L. Jeon, *Lab Chip* **2016**, *16*, 4189; b) S. Kim, M. Chung, N. L. Jeon, *Biomaterials* **2016**, *78*, 115.
- [43] E. C. Costa, A. F. Moreira, D. de Melo-Diogo, V. M. Gaspar, M. P. Carvalho, I. J. Correia, *Biotechnol. Adv.* **2016**, *34*, 1427.
- [44] a) D. Shweiki, M. Neeman, A. Itin, E. Keshet, *Proc. Natl. Acad. Sci. USA* **1995**, *92*, 768; b) K. Klimkiewicz, K. Węglarczyk, G. Collet, M. Paprocka, A. Guichard, M. Sarna, A. Jozkowicz, J. Dulak, T. Sarna, C. Grillon, *Cancer Lett.* **2017**, *396*, 10; c) X. Gong, C. Lin, J. Cheng, J. Su, H. Zhao, T. Liu, X. Wen, P. Zhao, *PLoS One* **2015**, *10*, e0130348; d) J. H. Kim, P. Verwilt, M. Won, J. Lee, J. L. Sessler, J. Han, J. S. Kim, *J. Am. Chem. Soc.* **2021**, *143*, 14115.
- [45] A. S. Nunes, A. S. Barros, E. C. Costa, A. F. Moreira, I. J. Correia, *Biotechnol. Bioeng.* **2019**, *116*, 206.
- [46] J. Ward, J. King, *Comput. Math. Methods Med.* **1999**, *1*, 287.
- [47] D. Hanahan, L. M. Coussens, *Cancer Cell* **2012**, *21*, 309.
- [48] G. Mehta, A. Y. Hsiao, M. Ingram, G. D. Luker, S. Takayama, *J. Controlled Release* **2012**, *164*, 192.
- [49] a) M. Ravi, V. Paramesh, S. Kaviya, E. Anuradha, F. P. Solomon, *J. Cell. Physiol.* **2015**, *230*, 16; b) K. M. Yamada, E. Cukierman, *Cell* **2007**, *130*, 601.
- [50] a) L. Ferreira, V. Gaspar, J. Mano, *Acta Biomater.* **2018**, *75*, 11; b) S. Nath, G. R. Devi, *Pharmacol. Ther.* **2016**, *163*, 94.
- [51] M. V. Monteiro, L. P. Ferreira, M. Rocha, V. M. Gaspar, J. F. Mano, *Biomaterials* **2022**, *287*, 121653.
- [52] J. Rodrigues, M. A. Heinrich, L. M. Teixeira, J. Prakash, *Trends Cancer* **2021**, *7*, 249.
- [53] H. Li, P. Liu, G. Kaur, X. Yao, M. Yang, *Adv. Healthcare Mater.* **2017**, *6*, 1700185.
- [54] A. A. Popova, T. Tronser, K. Demir, P. Haitz, K. Kuodyte, V. Starkuviene, P. Wajda, P. A. Levkin, *Small* **2019**, *15*, 1901299.
- [55] Y. Xia, H. Chen, J. Li, H. Hu, Q. Qian, R.-X. He, Z. Ding, S.-S. Guo, *ACS Appl. Mater. Interfaces* **2021**, *13*, 23489.
- [56] a) B. L. Khoo, G. Greci, T. Jing, Y. B. Lim, S. C. Lee, J. P. Thiery, J. Han, C. T. Lim, *Sci. Adv.* **2016**, *2*, e1600274; b) B. L. Khoo, G. Greci, Y. B. Lim, S. C. Lee, J. Han, C. T. Lim, *Nat. Protoc.* **2018**, *13*, 34.
- [57] W. Li, Y. Zhou, Y. Deng, B. L. Khoo, *Cancers* **2022**, *14*, 818.
- [58] X. Jiang, L. Ren, P. Tebon, C. Wang, X. Zhou, M. Qu, J. Zhu, H. Ling, S. Zhang, Y. Xue, *Small* **2021**, *17*, 2004282.
- [59] S. Goodarzi, A. Prunet, F. Rossetti, G. Bort, O. Tillement, E. Porcel, S. Lacombe, T.-D. Wu, J.-L. Guerquin-Kern, H. Delanoë-Ayari, *Lab Chip* **2021**, *21*, 2495.
- [60] a) J. Casey, X. Yue, T. D. Nguyen, A. Acun, V. R. Zellmer, S. Zhang, P. Zorlutuna, *Biomed. Mater.* **2017**, *12*, 025009; b) X. Yue, T. D. Nguyen, V. Zellmer, S. Zhang, P. Zorlutuna, *Biomaterials* **2018**, *170*, 37.
- [61] Q. Luan, J. H. Becker, C. Macaraniag, M. G. Massad, J. Zhou, T. Shimamura, I. Papautsky, *Lab Chip* **2022**, *22*, 2364.
- [62] S. Singh, L. A. Ray, P. Shahi Thakuri, S. Tran, M. C. Konopka, G. D. Luker, H. Tavana, *Biomaterials* **2020**, *238*, 119853.
- [63] A. Boussommier-Calleja, *Bioengineering Innovative Solutions for Cancer*, Elsevier, New York **2020**, p. 273.
- [64] O. Chaudhuri, S. T. Koshy, C. Branco da Cunha, J.-W. Shin, C. S. Verbeke, K. H. Allison, D. J. Mooney, *Nat. Mater.* **2014**, *13*, 970.
- [65] J. Liu, Y. Tan, H. Zhang, Y. Zhang, P. Xu, J. Chen, Y.-C. Poh, K. Tang, N. Wang, B. Huang, *Nat. Mater.* **2012**, *11*, 734.
- [66] a) K. M. Charoen, B. Fallica, Y. L. Colson, M. H. Zaman, M. W. Grinstaff, *Biomaterials* **2014**, *35*, 2264; b) C. S. Szot, C. F. Buchanan, J. W. Freeman, M. N. Rylander, *Biomaterials* **2011**, *32*, 7905; c) S.-Y. Jeong, J.-H. Lee, Y. Shin, S. Chung, H.-J. Kuh, *PLoS One* **2016**, *11*, e0159013.
- [67] P. Sabhachandani, V. Motwani, N. Cohen, S. Sarkar, V. Torchilin, T. Konry, *Lab Chip* **2016**, *16*, 497.
- [68] a) I. B. Fridman, G. S. Ugolini, V. VanDelinder, S. Cohen, T. Konry, *Biofabrication* **2021**, *13*, 035037; b) P. Sabhachandani, S. Sarkar, S. Mckenney, D. Ravi, A. M. Evens, T. Konry, *J. Controlled Release* **2019**, *295*, 21.
- [69] a) T. Zhang, Y. Deng, S. L. Yang, S. L. Chua, B. Z. Tang, B. L. Khoo, *Chem. Eng. J.* **2022**, *447*, 137579; b) Y. Deng, S. Y. Liu, S. L. Chua, B. L. Khoo, *Biosens. Bioelectron.* **2021**, *180*, 113113.
- [70] D. Loessner, K. S. Stok, M. P. Lutolf, D. W. Huttmacher, J. A. Clements, S. C. Rizzi, *Biomaterials* **2010**, *31*, 8494.
- [71] C. L. Hedegaard, C. Redondo-Gómez, B. Y. Tan, K. W. Ng, D. Loessner, A. Mata, *Sci. Adv.* **2020**, *6*, eabb3298.
- [72] P. Agarwal, H. Wang, M. Sun, J. Xu, S. Zhao, Z. Liu, K. J. Gooch, Y. Zhao, X. Lu, X. He, *ACS Nano* **2017**, *11*, 6691.
- [73] F. Xie, L. Sun, Y. Pang, G. Xu, B. Jin, H. Xu, X. Lu, Y. Xu, S. Du, Y. Wang, *Biomaterials* **2021**, *265*, 120416.
- [74] P. A. Johnson, S. Menegatti, A. C. Chambers, D. Alibhai, T. J. Collard, A. C. Williams, H. Bayley, A. W. Perriman, *Biofabrication* **2022**, *15*, 014103.
- [75] S. Mao, J. He, Y. Zhao, T. Liu, F. Xie, H. Yang, Y. Mao, Y. Pang, W. Sun, *Biofabrication* **2020**, *12*, 045014.
- [76] Y. Li, N. Khuu, E. Prince, H. Tao, N. Zhang, Z. Chen, A. Gevorkian, A. P. McGuigan, E. Kumacheva, *Biomacromolecules* **2021**, *22*, 419.
- [77] A. D. Arya, P. M. Hallur, A. G. Karkisaval, A. Gudipati, S. Rajendiran, V. Dhavale, B. Ramachandran, A. Jayaprakash, N. Gundiah, A. Chaubey, *ACS Appl. Mater. Interfaces* **2016**, *8*, 22005.
- [78] L. P. Ferreira, V. M. Gaspar, L. Mendes, I. F. Duarte, J. F. Mano, *Biomaterials* **2021**, *275*, 120983.
- [79] X. Ma, C. Yu, P. Wang, W. Xu, X. Wan, C. S. E. Lai, J. Liu, A. Koroleva-Maharajh, S. Chen, *Biomaterials* **2018**, *185*, 310.
- [80] a) K. Haase, G. S. Offeddu, M. R. Gillrie, R. D. Kamm, *Adv. Funct. Mater.* **2020**, *30*, 2002444; b) J. Paek, S. E. Park, Q. Lu, K. T. Park, M. Cho, J. M. Oh, K. W. Kwon, Y. S. Yi, J. W. Song, H. I. Edelstein,

- J. Ishibashi, W. Yang, J. W. Myerson, R. Y. Kiseleva, P. Aprelev, E. D. Hood, D. Stambolian, P. Seale, V. R. Muzykantor, D. Huh, *ACS Nano* **2019**, *13*, 7627.
- [81] Y. Nashimoto, R. Okada, S. Hanada, Y. Arima, K. Nishiyama, T. Miura, R. Yokokawa, *Biomaterials* **2020**, *229*, 119547.
- [82] D. Tuveson, H. Clevers, *Science* **2019**, *364*, 952.
- [83] R. Shi, N. Radulovich, C. Ng, N. Liu, H. Notsuda, M. Cabanero, S. N. Martins-Filho, V. Raghavan, Q. Li, A. S. Mer, *Clin. Cancer Res.* **2020**, *26*, 1162.
- [84] N. Sachs, J. de Ligt, O. Kopper, E. Gogola, G. Bounova, F. Weeber, A. V. Balgobind, K. Wind, A. Gracanin, H. Begthel, *Cell* **2018**, *172*, 373.
- [85] S. F. Boj, C.-I. Hwang, L. A. Baker, I. I. C. Chio, D. D. Engle, V. Corbo, M. Jager, M. Ponz-Sarvise, H. Tiriari, M. S. Spector, *Cell* **2015**, *160*, 324.
- [86] M. Van de Wetering, H. E. Francies, J. M. Francis, G. Bounova, F. Iorio, A. Pronk, W. van Houdt, J. van Gorp, A. Taylor-Weiner, L. Kester, *Cell* **2015**, *161*, 933.
- [87] O. Kopper, C. J. De Witte, K. Löhmussaar, J. E. Valle-Inclan, N. Hani, L. Kester, A. V. Balgobind, J. Korving, N. Proost, H. Begthel, *Nat. Med.* **2019**, *25*, 838.
- [88] D. Gao, I. Vela, A. Sboner, P. J. Iaquina, W. R. Karthaus, A. Gopalan, C. Dowling, J. N. Wanjala, E. A. Undvall, V. K. Arora, *Cell* **2014**, *159*, 176.
- [89] S. Bartfeld, T. Bayram, M. van de Wetering, M. Huch, H. Begthel, P. Kujala, R. Vries, P. J. Peters, H. Clevers, *Gastroenterology* **2015**, *148*, 126.
- [90] G. Vlachogiannis, S. Hedayat, A. Vatsiou, Y. Jamin, J. Fernández-Mateos, K. Khan, A. Lampis, K. Eason, I. Huntingford, R. Burke, *Science* **2018**, *359*, 920.
- [91] B. M. Larsen, M. Kannan, L. F. Langer, B. D. Leibowitz, A. Bentaieb, A. Cancino, I. Dolgalev, B. E. Drummond, J. R. Dry, C.-S. Ho, *Cell Rep.* **2021**, *36*, 109429.
- [92] S. Ding, C. Hsu, Z. Wang, N. R. Natesh, R. Millen, M. Negrete, N. Giroux, G. O. Rivera, A. Dohlman, S. Bose, *Cell Stem Cell* **2022**, *29*, 905.
- [93] S. Jiang, H. Zhao, W. Zhang, J. Wang, Y. Liu, Y. Cao, H. Zheng, Z. Hu, S. Wang, Y. Zhu, *Cell Rep. Med.* **2020**, *1*, 100161.
- [94] S. Ng, W. J. Tan, M. M. X. Pek, M.-H. Tan, M. Kurisawa, *Biomaterials* **2019**, *219*, 119400.
- [95] C. R. Below, J. Kelly, A. Brown, J. D. Humphries, C. Hutton, J. Xu, B. Y. Lee, C. Cintas, X. Zhang, V. Hernandez-Gordillo, *Nat. Mater.* **2022**, *21*, 110.
- [96] E. Prince, J. Cruickshank, W. Ba-Alawi, K. Hodgson, J. Haight, C. Tobin, A. Wakeman, A. Avoulov, V. Topolskaia, M. J. Elliott, *Nat. Commun.* **2022**, *13*, 1466.
- [97] A. Mazzocchi, M. Devarasetty, S. Herberg, W. J. Petty, F. Marini, L. Miller, G. Kucera, D. K. Dukes, J. Ruiz, A. Skardal, *ACS Biomater. Sci. Eng.* **2019**, *5*, 1937.
- [98] D. Osuna de la Peña, S. M. D. Trabulo, E. Collin, Y. Liu, S. Sharma, M. Tatari, D. Behrens, M. Erkan, R. T. Lawlor, A. Scarpa, C. Heeschen, A. Mata, D. Loessner, *Nat. Commun.* **2021**, *12*, 5623.
- [99] a) S. Kim, S. Min, Y. S. Choi, S. H. Jo, J. H. Jung, K. Han, J. Kim, S. An, Y. W. Ji, Y. G. Kim, S. W. Cho, *Nat. Commun.* **2022**, *13*, 1692; b) P. A. Mollica, E. N. Booth-Creech, J. A. Reid, M. Zamponi, S. M. Sullivan, X.-L. Palmer, P. C. Sachs, R. D. Bruno, *Acta Biomater.* **2019**, *95*, 201.
- [100] G. S. van Tienderen, O. Rosmark, R. Lieshout, J. Willems, F. de Weijer, L. E. Rendin, G. Westergren-Thorsson, M. Doukas, B. G. Koerkamp, M. E. van Royen, *Acta Biomater.* **2023**, *158*, 115.
- [101] N. Brandenburg, S. Hoehnel, F. Kuttler, K. Homicsko, C. Ceroni, T. Ringel, N. Gjorevski, G. Schwank, G. Coukos, G. Turcatti, *Nat. Biomed. Eng.* **2020**, *4*, 863.
- [102] a) A.-N. Cho, Y. Jin, Y. An, J. Kim, Y. S. Choi, J. S. Lee, J. Kim, W.-Y. Choi, D.-J. Koo, W. Yu, G.-E. Chang, D.-Y. Kim, S.-H. Jo, J. Kim, S.-Y. Kim, Y.-G. Kim, J. Y. Kim, N. Choi, E. Cheong, Y.-J. Kim, H. S. Je, H.-C. Kang, S.-W. Cho, *Nat. Commun.* **2021**, *12*, 473; b) G. Fang, H. Lu, R. Al-Nakashli, R. Chapman, Y. Zhang, L. A. Ju, G. Lin, M. H. Stenzel, D. Jin, *Biofabrication* **2021**, *14*, 015006.
- [103] T. H. Shin, M. Kim, C. O. Sung, S. J. Jang, G. S. Jeong, *Lab Chip* **2019**, *19*, 3664.
- [104] V. S. Shirure, Y. Bi, M. B. Curtis, A. Lezia, M. M. Goedegebuure, S. P. Goedegebuure, R. Aft, R. C. Fields, S. C. George, *Lab Chip* **2018**, *18*, 3687.
- [105] B. Schuster, M. Junkin, S. S. Kashaf, I. Romero-Calvo, K. Kirby, J. Matthews, C. R. Weber, A. Rzhetsky, K. P. White, S. Tay, *Nat. Commun.* **2020**, *11*, 5271.
- [106] E. Prince, S. Kheiri, Y. Wang, F. Xu, J. Cruickshank, V. Topolskaia, H. Tao, E. W. Young, A. P. McGuigan, D. W. Cescon, *Adv. Healthcare Mater.* **2022**, *11*, 2101085.
- [107] a) L. Horowitz, A. Rodriguez, Z. Dereli-Korkut, R. Lin, K. Castro, A. Mikheev, R. Monnat, A. Folch, R. C. Rostomily, *NPJ Precis Oncol* **2020**, *4*, 12; b) A. Rodriguez, L. Horowitz, K. Castro, H. Kenerson, N. Bhattacharjee, G. Gandhe, A. Raman, R. Monnat, R. Yeung, R. Rostomily, *Lab Chip* **2020**, *20*, 1658.
- [108] L. F. Horowitz, A. D. Rodriguez, A. Au-Yeung, K. W. Bishop, L. A. Barner, G. Mishra, A. Raman, P. Delgado, J. T. Liu, T. S. Gujral, *Lab Chip* **2021**, *21*, 122.
- [109] B. Blanco-Fernandez, V. M. Gaspar, E. Engel, J. F. Mano, *Adv. Sci.* **2021**, *8*, 2003129.
- [110] a) V. Murlidhar, R. M. Reddy, S. Fouladdel, L. Zhao, M. K. Ishikawa, S. Grabauskiene, Z. Zhang, J. Lin, A. C. Chang, P. Carrott, *Cancer Res.* **2017**, *77*, 5194; b) Y. Zhou, B. Wang, J. Wu, C. Zhang, Y. Zhou, X. Yang, J. Zhou, W. Guo, J. Fan, *BMC Cancer* **2016**, *16*, 506.
- [111] D. Hanahan, R. A. Weinberg, *Cell* **2011**, *144*, 646.
- [112] S. Kim, H. Lee, M. Chung, N. L. Jeon, *Lab Chip* **2013**, *13*, 1489.
- [113] C. P. Miller, C. Tsuchida, Y. Zheng, J. Himmelfarb, S. Akilesh, *Neoplasia* **2018**, *20*, 610.
- [114] a) J. Bai, K. Haase, J. J. Roberts, J. Hoffmann, H. T. Nguyen, Z. Wan, S. Zhang, B. Sarker, N. Friedman, C. Ristic-Lehmann, R. D. Kamm, *Biomaterials* **2021**, *268*, 120592; b) J. A. Jiménez-Torres, S. L. Peery, K. E. Sung, D. J. Beebe, *Adv. Healthcare Mater.* **2016**, *5*, 198; c) D.-H. T. Nguyen, S. C. Stapleton, M. T. Yang, S. S. Cha, C. K. Choi, P. A. Galie, C. S. Chen, *Proc. Natl. Acad. Sci. USA* **2013**, *110*, 6712.
- [115] K. Jeong, Y. J. Yu, J. Y. You, W. J. Rhee, J. A. Kim, *Lab Chip* **2020**, *20*, 548.
- [116] S. Lee, S. Kim, D. J. Koo, J. Yu, H. Cho, H. Lee, J. M. Song, S. Y. Kim, D. H. Min, N. L. Jeon, *ACS Nano* **2021**, *15*, 338.
- [117] D. D. Truong, A. Kratz, J. G. Park, E. S. Barrientos, H. Saini, T. Nguyen, B. Pockaj, G. Mouneimne, J. LaBaer, M. Nikkhah, *Cancer Res.* **2019**, *79*, 3139.
- [118] K. M. Lugo-Cintrón, M. M. Gong, J. M. Ayuso, L. A. Tomko, D. J. Beebe, M. Virumbrales-Muñoz, S. M. Ponik, *Cancers* **2020**, *12*, 1173.
- [119] Z. Du, S. Mi, X. Yi, Y. Xu, W. Sun, *Biofabrication* **2018**, *10*, 034102.
- [120] S. Nagaraju, D. Truong, G. Mouneimne, M. Nikkhah, *Adv. Healthcare Mater.* **2018**, *7*, 1701257.
- [121] D. Truong, R. Fiorelli, E. S. Barrientos, E. L. Melendez, N. Sanai, S. Mehta, M. Nikkhah, *Biomaterials* **2019**, *198*, 63.
- [122] R. Li, J. D. Hebert, T. A. Lee, H. Xing, A. Boussommier-Calleja, R. O. Hynes, D. A. Lauffenburger, R. D. Kamm, *Cancer Res.* **2017**, *77*, 279.
- [123] V. Surendran, D. Rutledge, R. Colmon, A. Chandrasekaran, *Biofabrication* **2021**, *13*, 035029.
- [124] W. Sun, Y. Chen, Y. Wang, P. Luo, M. Zhang, H. Zhang, P. Hu, *Analyt.* **2018**, *143*, 5431.
- [125] D. Truong, J. Puleo, A. Llave, G. Mouneimne, R. D. Kamm, M. Nikkhah, *Sci. Rep.* **2016**, *6*, 34094.
- [126] A. S. Piotrowski-Daspit, J. Tien, C. M. Nelson, *Integr. Biol.* **2016**, *8*, 319.

- [127] I. K. Zervantonakis, S. K. Hughes-Alford, J. L. Charest, J. S. Condeelis, F. B. Gertler, R. D. Kamm, *Proc. Natl. Acad. Sci. USA* **2012**, *109*, 13515.
- [128] A. Boussommier-Calleja, Y. Atiyas, K. Haase, M. Headley, C. Lewis, R. D. Kamm, *Biomaterials* **2019**, *198*, 180.
- [129] M. Crippa, S. Bersini, M. Gilardi, C. Arrigoni, S. Gamba, A. Falanga, C. Candrian, G. Dubini, M. Vanoni, M. Moretti, *Lab Chip* **2021**, *21*, 1061.
- [130] C. Hajal, L. Ibrahim, J. C. Serrano, G. S. Offeddu, R. D. Kamm, *Biomaterials* **2021**, *265*, 120470.
- [131] M. Humayun, J. M. Ayuso, R. A. Brenneke, M. Virumbrales-Muñoz, K. Lugo-Cintrón, S. Kerr, S. M. Ponik, D. J. Beebe, *Biomaterials* **2021**, *270*, 120640.
- [132] J. S. Jeon, S. Bersini, M. Gilardi, G. Dubini, J. L. Charest, M. Moretti, R. D. Kamm, *Proc. Natl. Acad. Sci. USA* **2015**, *112*, 214.
- [133] T. J. Kwak, E. Lee, *Biofabrication* **2020**, *13*, 015002.
- [134] C. Hajal, Y. Shin, L. Li, J. C. Serrano, T. Jacks, R. D. Kamm, *Sci. Adv.* **2021**, *7*, eabg8139.
- [135] N. Peela, E. Barrientos, D. Truong, G. Mouneimne, M. Nikkhah, *Integr. Biol.* **2017**, *9*, 988.
- [136] S. Y. Jeong, J. H. Lee, Y. Shin, S. Chung, H. J. Kuh, *PLoS One* **2016**, *11*, e0159013.
- [137] F. Eduati, R. Utharala, D. Madhavan, U. P. Neumann, T. Longerich, T. Cramer, J. Saez-Rodriguez, C. A. Merten, *Nat. Commun.* **2018**, *9*, 23434.
- [138] J. A. Jimenez-Torres, M. Virumbrales-Munoz, K. E. Sung, M. H. Lee, E. J. Abel, D. J. Beebe, *EBioMedicine* **2019**, *42*, 408.
- [139] M. Virumbrales-Muñoz, J. Chen, J. Ayuso, M. Lee, E. J. Abel, D. J. Beebe, *Lab Chip* **2020**, *20*, 4420.
- [140] E. Ivanova, M. Kuraguchi, M. Xu, A. J. Portell, L. Taus, I. Diala, A. S. Lalani, J. Choi, E. S. Chambers, S. Li, *Clin. Cancer Res.* **2020**, *26*, 2393.
- [141] K. M. Lugo-Cintrón, J. M. Ayuso, M. Humayun, M. M. Gong, S. C. Kerr, S. M. Ponik, P. M. Harari, M. Virumbrales-Munoz, D. J. Beebe, *EBioMedicine* **2021**, *73*, 103634.
- [142] a) S. Y. Qin, A. Q. Zhang, X. Z. Zhang, *Small* **2018**, *14*, 1802417; b) X. Gao, L. Li, X. Cai, Q. Huang, J. Xiao, Y. Cheng, *Biomaterials* **2021**, *265*, 120404.
- [143] H. Maeda, H. Nakamura, J. Fang, *Adv. Drug Delivery Rev.* **2013**, *65*, 71.
- [144] H. F. Wang, R. Ran, Y. Liu, Y. Hui, B. Zeng, D. Chen, D. A. Weitz, C. X. Zhao, *ACS Nano* **2018**, *12*, 11600.
- [145] A. Oddo, B. Peng, Z. Tong, Y. Wei, W. Y. Tong, H. Thissen, N. H. Voelcker, *Trends Biotechnol.* **2019**, *37*, 1295.
- [146] H. Xu, Z. Li, Y. Yu, S. Sizzdahkhani, W. S. Ho, F. Yin, L. Wang, G. Zhu, M. Zhang, L. Jiang, *Sci. Rep.* **2016**, *6*, 36670.
- [147] G. Adriani, D. Ma, A. Pavesi, R. D. Kamm, E. L. Goh, *Lab Chip* **2017**, *17*, 448.
- [148] S. Bang, S.-R. Lee, J. Ko, K. Son, D. Takh, J. Ahn, C. Im, N. L. Jeon, *Sci. Rep.* **2017**, *7*, 8083.
- [149] D. E. Eigenmann, G. Xue, K. S. Kim, A. V. Moses, M. Hamburger, M. Oufir, *Fluids Barriers CNS* **2013**, *10*, 33.
- [150] E. A. Winkler, R. D. Bell, B. V. Zlokovic, *Nat. Neurosci.* **2011**, *14*, 1398.
- [151] S. Lee, M. Chung, S. R. Lee, N. L. Jeon, *Biotechnol. Bioeng.* **2020**, *117*, 748.
- [152] M. Campisi, Y. Shin, T. Osaki, C. Hajal, V. Chiono, R. D. Kamm, *Biomaterials* **2018**, *180*, 117.
- [153] D. Truong, R. Fiorelli, E. S. Barrientos, E. L. Melendez, N. Sanai, S. Mehta, M. Nikkhah, *Biomaterials* **2019**, *198*, 63.
- [154] L. Lin, Z. He, M. Jie, J.-M. Lin, J. Zhang, *Talanta* **2021**, *234*, 122702.
- [155] E. A. Adjei-Sowah, S. A. O'Connor, J. Veldhuizen, C. Lo Cascio, C. Plaisier, S. Mehta, M. Nikkhah, *Adv. Sci.* **2022**, *9*, 2201436.
- [156] M. Altemus, B. Leung, A. Morikawa, M. Dziubinski, M. Castro, S. Merajver, *Cancer Res.* **2016**, *76*, 1700.
- [157] S. W. L. Lee, M. Campisi, T. Osaki, L. Possenti, C. Mattu, G. Adriani, R. D. Kamm, V. Chiono, *Adv. Healthcare Mater.* **2020**, *9*, 1901486.
- [158] J. P. Straehla, C. Hajal, H. C. Safford, G. S. Offeddu, N. Boehnke, T. G. Dacoba, J. Wyckoff, R. D. Kamm, P. T. Hammond, *Proc. Natl. Acad. Sci. USA* **2022**, *119*, e2118697119.
- [159] S. Seo, S. Y. Nah, K. Lee, N. Choi, H. N. Kim, *Adv. Funct. Mater.* **2022**, *32*, 2106860.
- [160] X. Cui, C. Ma, V. Vasudevaraja, J. Serrano, J. Tong, Y. Peng, M. De-lorenzo, G. Shen, J. Frenster, R.-T. T. Morales, *Elife* **2020**, *9*, e52253.
- [161] a) H.-G. Yi, Y. H. Jeong, Y. Kim, Y.-J. Choi, H. E. Moon, S. H. Park, K. S. Kang, M. Bae, J. Jang, H. Youn, *Nat. Biomed. Eng.* **2019**, *3*, 509; b) C. Li, S. Li, K. Du, P. Li, B. Qiu, W. Ding, *ACS Appl. Mater. Interfaces* **2021**, *13*, 19768; c) M. Tang, S. K. Tiwari, K. Agrawal, M. Tan, J. Dang, T. Tam, J. Tian, X. Wan, J. Schimelman, S. You, *Small* **2021**, *17*, 2006050.
- [162] J. Willemsse, G. van Tienderen, E. van Hengel, I. Schurink, D. van der Ven, Y. Kan, P. de Ruyter, O. Rosmark, K. Schneeberger, B. van der Eerden, *Biomaterials* **2022**, *284*, 121473.
- [163] J. Schrader, T. T. Gordon-Walker, R. L. Aucott, M. van Deemter, A. Quaas, S. Walsh, D. Bente, S. J. Forbes, R. G. Wells, J. P. Iredale, *Hepatology* **2011**, *53*, 1192.
- [164] S. Sinha, M. Ayushman, X. Tong, F. Yang, *Adv. Healthcare Mater.* **2022**, 2202147.
- [165] M. Yu, A. Bardia, N. Aceto, F. Bersani, M. W. Madden, M. C. Donaldson, R. Desai, H. Zhu, V. Comaills, Z. Zheng, *Science* **2014**, *345*, 216.
- [166] J. Lee, S. Mehrotra, E. Zare-Eelanjegh, R. O. Rodrigues, A. Akbarinejad, D. Ge, L. Amato, K. Kiaee, Y. Fang, A. Rosenkranz, *Small* **2021**, *17*, 2004258.
- [167] Z. Xu, E. Li, Z. Guo, R. Yu, H. Hao, Y. Xu, Z. Sun, X. Li, J. Lyu, Q. Wang, *ACS Appl. Mater. Interfaces* **2016**, *8*, 25840.



Wenxiu Li is a Ph.D. student at the Department of Biomedical Sciences at City University of Hong Kong. She received her M.Sc. degree in materials science from South China University of Technology in 2015. Her research interests include the development of biomimetic in vitro cancer models using tissue engineering technologies for drug discovery and cancer biology.



Mengsu Yang is currently vice-president (Research and Technology), Yeung Kin-Man Chair Professor of Biomedical Sciences, and Directors of the Tung Biomedical Sciences Centre at the City University of Hong Kong. He has published over 280 peer-reviewed scientific papers and 33 American and Chinese patents. His research interests focus on studying cancer biology and developing biochips and nanotechnology for diagnostics and therapeutic applications.